

**Key Words:** Saltstone PA,  
Concrete Degradation,  
Concrete Properties,  
Saltstone Properties,  
Concrete Test Methods

**Retention:** Permanent

**EVALUATION OF SULFATE ATTACK ON  
SALTSTONE VAULT CONCRETE AND SALTSTONE**

**PART II: TEST METHODS TO SUPPORT MOISTURE AND IONIC  
TRANSPORT MODELING USING THE STADIUM<sup>®</sup> CODE**

**SIMCO TECHNOLOGIES, INC.  
SUBCONTRACT SIMCORD08009 ORDER AC48992N (U)**

**Christine A. Langton**

**AUGUST 19, 2008**

**Savannah River National Laboratory  
Savannah River Nuclear Solutions, LLC  
Aiken, SC 29808**

**Prepared for the U.S. Department of Energy  
Under Contract No. DE- AC09-08SR22470**



**SRNL**  
SAVANNAH RIVER NATIONAL LABORATORY

**DISCLAIMER**

This work was prepared under an agreement with and funded by the U.S. Government. Neither the U.S. Government or its employees, nor any of its contractors, subcontractors or their employees, makes any express or implied: 1. warranty or assumes any legal liability for the accuracy, completeness, or for the use or results of such use of any information, product, or process disclosed; or 2. representation that such use or results of such use would not infringe privately owned rights; or 3. endorsement or recommendation of any specifically identified commercial product, process, or service. Any views and opinions of authors expressed in this work do not necessarily state or reflect those of the United States Government, or its contractors, or subcontractors.

This document was prepared in conjunction with work accomplished under Contract No. DE-AC09-08SR22470 with the U.S. Department of Energy.

**Printed in the United States of America**

**Prepared For  
U.S. Department of Energy**

**Key Words:** Saltstone PA,  
Concrete Degradation,  
Concrete Properties,  
Saltstone Properties,  
Concrete Test Methods

**Retention:** Permanent

**EVALUATION OF SULFATE ATTACK ON  
SALTSTONE VAULT CONCRETE AND SALTSTONE**

**PART II: TEST METHODS TO SUPPORT MOISTURE AND  
IONIC TRANSPORT MODELING USING THE STADIUM<sup>®</sup> CODE**

**SIMCO TECHNOLOGIES, INC.  
SUBCONTRACT SIMCORD08009 ORDER AC48992N (U)**

**C. A. Langton**

**Savannah River National Laboratory  
Savannah River Nuclear Solutions, LLC  
Aiken, SC 29809**

**August 19, 2008**

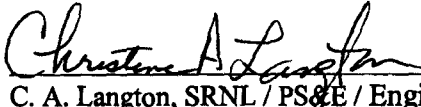
**Savannah River National Laboratory  
Savannah River Nuclear Solutions, LLC  
Aiken, SC 29808**

**Prepared for the U.S. Department of Energy  
Under Contract No. DE- AC09-08SR22470**



**REVIEWS AND APPROVALS**


**Authors:**


  
C. A. Langton, SRNL / PS&E / Engineering Process Development 10-26-08  
Date

**Technical Reviewer:**

  
G. P. Flach, SRNL / Geo-Modeling 10/29/08  
Date


**SRNL Management Approvals:**

  
H. H. Burns, Project Manager, SRNL / PS&E 10/31/08  
Date

  
A. B. Barnes, Manager, SRNL / PS&E 10/31/08  
Date

  
J. C. Griffin, Manager, SRNL / E&CPT 10/31/08  
Date

**Customer Approvals:**

  
J. L. Newman, REG INTEGRATION & ENV SERVICES 11/5/08  
Date

  
T. Robinson, REG INTEGRATION & ENV SERVICES 11/11/08  
Date

## TABLE OF CONTENTS

<b>Reviews and Approvals</b> .....	<b>i</b>
<b>Table of Contents</b> .....	<b>ii</b>
<b>List of Acronyms</b> .....	<b>iii</b>
<b>1.0 EXECUTIVE SUMMARY</b> .....	<b>1</b>
<b>2.0 INTRODUCTION</b> .....	<b>3</b>
2.1 Objective.....	3
2.2 Background.....	3
2.3 Standard Concrete Preparation and Characterization Test.....	4
<b>3.0 MOISTURE AND IONIC TRANSPORT CHARACTERIZATION</b>	
<b>METHODOLOGY</b> .....	<b>5</b>
3.1 Ion Migration Test.....	5
3.2 Drying / Absorption Test Water Diffusivity Determination .....	6
3.3 Adsorption – Desorption Isotherm Test .....	7
3.4 Concrete Immersion Test.....	8
3.5 Pore Solution Extraction Test.....	8
<b>4.0 REFERENCES</b> .....	<b>8</b>
<b>5.0 ATTACHMENT 1.</b>	
<b>SUMMARY OF SUBCONTRACT NO. AC 48992N WORK REQUIREMENTS.A1-1</b>	
<b>6.0 ATTACHMENT 2.</b>	
<b>TEST METHODS FOR CHARACTERIZING TRANSPORT PROPERTIES OF</b>	
<b>CONCRETE TO SUPPORT THE STADIUM<sup>®</sup> SERVICE LIFE PREDICTION</b>	
<b>CODE</b> .....	<b>A2-1</b>
<b>APPENDIX A. Assembly of Migration Cells</b> .....	<b>A2-25</b>
<b>APPENDIX B. Making Solutions for Migration Test</b> .....	<b>A2-27</b>
<b>APPENDIX C. Accompanying Specimen for Pore Solution Extraction</b> .....	<b>A2-29</b>
<b>APPENDIX D. Recent Advances in the Determination of Ionic Diffusion</b>	
<b>Coefficients Using Migration Test Results</b> .....	<b>A2-31</b>
<b>APPENDIX E. Determination of the Water Diffusivity of Concrete Using</b>	
<b>Drying/Absorption Test Results</b> .....	<b>A2-49</b>

## List of Acronyms

ASTM	American Society for Testing & Materials
C-S-H	Calcium silicate hydrate (poorly crystalline solid)
E&CPT	Engineering and Chemical Processing Technology
PA	Performance Assessment
PS&E	Process Science and Engineering
RH	Relative Humidity
SIMCO	SIMCO Technologies, Inc.
SRNL	Savannah River National Laboratory
SRNS	Savannah River Nuclear Solutions
SRS	Savannah River Site
STR	Subcontract Technical Representative
TTR	Technical Task Request
WSRC	Washington Savannah River Company

## 1.0 EXECUTIVE SUMMARY

This report summarizes test methods used by SIMCO Technologies, Inc., to characterize moisture and ionic transport through cured concrete, in particular through samples of the saltstone vault 1 / 4 concrete, vault 2 concrete, and the saltstone waste form. Transport properties<sup>1</sup> determined by these methods were then used by SIMCO Technologies, Inc. to predict the service life of concrete structures using the STADIUM<sup>®</sup> Service Life Prediction Code which is a one-dimensional diffusion model.

This report is the cover letter for the Task 5 Submittal, Test Methodology, and provides a description of several of the specialized test methods used to characterize the samples prepared by SIMCO Technologies, Inc. Methods for the following tests are described in this report:

- Ion Migration Test (accelerated Cl<sup>-</sup> migration test to determine tortuosity)
- Drying (Desorption) / Adsorption Test (determine equilibrium moisture content at 50% relative humidity (RH) to determine A and B parameters in the Richards' equation)
- Adsorption –Desorption Test as a Function of Relative Humidity Test (determine equilibrium water contents over a range of relative humidities, i.e., over a range of water saturation)
- Concrete Immersion Test (provide data to validate the STADIUM<sup>®</sup> service life predictions)
- Pore Solution Extraction Test (extract and analyze saltstone and vault concrete pore solutions to provide a basis for simulating corrosive leachate compositions for service life predictions)

Procedures for preparing and curing samples and for ASTM or other standard methods are reported in SRNS-STI-2008-00050.

The work was requested by J. L. Newman, REG INTEGRATION & ENV SERVICES, and coordinated through H. H. Burns, PS&E / SRNL, and will support the 2008 Saltstone Performance Analysis [Burns, 2008] and implemented via Subcontract No. AC48992N. The overall objective of this subcontract was to evaluate the durability<sup>2</sup> of saltstone vault 1 / 4 and vault 2 concrete with respect to sulfate attack using the STADIUM<sup>®</sup> code.

Data generated from these tests will be used in the STADIUM<sup>®</sup> Service Life Prediction Code to determine the impact of exposure of saltstone and the saltstone vault concrete to SRS soil pore water, and to leachates generated by infiltrating water contacting the saltstone waste form material. Results of this evaluation will be used to support the Saltstone Performance Assessment.

---

<sup>1</sup> Moisture and ionic transport properties are referred to as hydraulic properties in SRS PA applications.

<sup>2</sup> Ability to provide diffusion controlled containment of radionuclides.

**BLANK PAGE**



## 2.0 INTRODUCTION

### 2.1 Objective

The objective of this report is to document test methods used by SIMCO Technologies, Inc. for characterizing moisture and ionic transport through cured concrete. Transport properties determined by these methods are used by SIMCO Technologies, Inc. to predict the service life of concrete structures using the Stadium code which is a one-dimensional diffusion model.

These test methods will be used to characterize Saltstone Vault 1 / 4 and Vault 2 concrete samples prepared by SIMCO Technologies as part of Subcontract No. AC 48992N. Work performed under this subcontract will evaluate the effect of alkaline sulfate solutions on the long-term performance (durability) of the vaults.

This work was requested by J. L. Newman, REG INTEGRATION & ENV SERVICES, and coordinated through H. H. Burns, PS&E / SRNL, and will support the 2008 Saltstone Performance Analysis [Burns, 2008].

### 2.2 Background

The saltstone waste form contains high concentrations of more or less soluble sulfate and aluminate. The waste form is cast as a slurry into concrete vaults which isolate the cured waste form from the environment. The performance of the waste form over the long term (10,000 years) is required for disposal of long lived radionuclides in the near surface environment.

The ability of the concrete vault to serve as a barrier between the environment (water in the environment) and source of mobile, water soluble radionuclides depends on how aging and exposure changes the permeability and water, gas and contaminant diffusivities of the concrete vault. (The vaults are part of a large landfill that will be covered by an engineered barrier that will limit infiltration of water during a portion of the performance time.)

A subcontract was awarded to SIMCO Technologies, Inc., to use existing expertise and simulation codes (STADIUM<sup>®</sup>) and methodology to predict the effects of sulfate and aluminate exposure (from saltstone, a cement waste form) on reinforced concrete, specifically SRS saltstone Vault 4 and 2 concrete, over 10,000 years. A summary of the requirements in the Statement of Work are provided in Attachment 1 [Contract No. SIMCORD08009, Order No. AC48992N, 2008].

Results of the study will be used as input to the Saltstone Performance Assessment, which predicts transport of radionuclides from the saltstone waste form into the surrounding environment and water table. In particular, they will be used to define assumptions for vault concrete degradation and should be sufficiently robust to withstand peer-review.

### **2.3 Standard Concrete Preparation and Characterization Test**

Monthly reports supplied by SIMCO Technologies, Inc. identify and include descriptions of test methods used for the following activities performed in support of this subcontract:

- Preparing Saltstone Vault 1 / 4 and Vault 2 concrete samples for physical and transport property characterization.
- Characterizing properties of fresh Saltstone Vault 1 / 4 concrete samples.
- Characterizing physical properties of cured Saltstone Vault 1 / 4 concrete samples.

### 3.0 MOISTURE AND IONIC TRANSPORT CHARACTERIZATION METHODOLOGY

#### 3.1 Ion Migration Test

The objective of this test is to determine the tortuosity of a concrete sample so that the intrinsic diffusion coefficients for various ions can be calculated using literature values for ionic diffusion coefficients in free water<sup>3</sup> and Equation 1.

$$\text{Equation 1.} \quad D_i = \tau D_i^0$$

Where:  $D_i$  = Diffusion coefficient for the ion in the pore water of the saturated porous material (m<sup>2</sup>/s)

$\tau$  = Tortuosity of void space in the saturated porous solid

$D_i^0$  = Diffusion coefficient of the ion in free water (m<sup>2</sup>/s)

Diffusion coefficients for most ions in free water are available in the reference literature. The information required to determine the diffusion coefficients of ions through the pore water of a saturated concrete sample are the tortuosity of the pores and influence of chemical binding (reduction in concentration of the ions in the pore solution as the result of chemical processes during the testing).

A modified version of the rapid (accelerated) chloride penetration test (modified ASTM C1202<sup>4</sup>) was used to determine the tortuosity and thereby diffusion coefficients of ionic species in the saltstone vault 1 / 4 and vault 2 concrete samples prepared at SIMCO Technologies, Inc. In this test Cl<sup>-</sup> migration through a wafer-shaped sample (thin disk) mounted between an upstream cell (filled with an alkaline chloride-containing electrolytic solution) and a down stream cell (filled with an alkaline solution without chloride) is accelerated by applying an electrical current through the cell. The negative electrode is connected to the upstream cell and the positive electrode is connected to the downstream cell. The current is monitored for 15 days.

Output from this test was used to calculate tortuosity by reproducing the current measured in the test with the STADIUM<sup>®</sup> model results and adjusting the STADIUM<sup>®</sup> output until the

---

<sup>3</sup>  $D_{\text{ionic}} = D_{\text{effective}}$  (Ionic diffusion coefficients in this report correspond to the effective diffusion coefficients reported in WSRC-STI-2006-00198 and in the SRS PAs.)

$D_{\text{effective}} = D_{\text{molecular diffusion in water}} \times \text{Tortuosity}$

$D_{\text{intrinsic}} = (D_{\text{effective}}) (\text{Porosity})$

<sup>4</sup> ASTM C1202 - Standard Test Method for Electrical Indication of Concrete's Ability to Resist Chloride Ion Penetration

sum of the ionic fluxes corresponds to the measured current. The Samson-Marchand analysis of the data generated in this test accounts for electrical coupling as well as chemical activity between ionic fluxes and is described in more detail in Attachment 2, Appendix D.

### 3.2 Drying / Absorption Test Water Diffusivity Determination

The objective of this test is to determine values for A and B<sup>5</sup> so that the water diffusivity can be estimated using Richards' water transport model assuming that the water diffusivity can be expressed as an exponential function shown in Equation 2.<sup>6</sup> A detailed explanation of the test method and calculations used to determine parameters A and B is provided in Attachment 2 Appendix E.

**Equation 2.**  $D_w = A \exp(Bw)$

Where:  $D_w$  = Water diffusivity (nonlinear)

$w$  = Volumetric water content

$A$  = Experimentally determined parameters

$B$  = Experimentally determined parameter (positive)

The water drying (desorption) test used by SIMCO technologies Inc. to determine the parameters A and B in Equation 2 is a new test developed by Samson, et al., and is based on drying initially saturated samples. Two sample thicknesses are used, 5 cm and 1 cm, are used in the test and drying takes place at 50 % RH. Weight loss is measured as a function of time until the masses of the 1 cm sample on four consecutive measurements are within 0.01g. The test period for concrete typically ranges from 40 (low quality concrete) to more than 70 days (blended cement concrete)

Analysis of the drying test results using Richards' equation, Equation 3, requires knowledge of the initial water content of the material. Samson et al., assume that since the sample is initially saturated, the water content (volume) corresponds to the porosity which they measure using the ASTM C 642 standard method for measuring the permeable voids in concrete.

**Equation 3.**  $\frac{\partial w}{\partial t} - \text{div}(D_w \text{grad}(w)) = 0$

---

<sup>5</sup> Analysis of the test results and simulations for numerous concrete mix designs indicated that the concrete mix design does not have a strong influence on the B parameter. In all cases the best fit B values ranged from 75 to 85.

Consequently a B value of 80 was selected for all concrete mix designs. Additional analyses suggested that the B value depends on the volume of cement paste in the concrete rather than on the mixture of cementitious materials used (i.e. portland cement or binary or ternary blends).

<sup>6</sup> Expressions for  $D_w$  based on a mechanistic description of fluid flow in unsaturated materials yield relationships involving multiple parameters such as the permeability, which are known to be difficult to evaluate in cementitious materials. Instead SIMCO Technologies Inc. uses a simplified nonlinear relationship proposed by Hall 1994. See Attachment 2 Appendix E.

Where:  $w$  = Volumetric water content ( $\text{cm}^3/\text{cm}^3$ )  
 $D_w$  = Water Diffusivity ( $\text{m}^2/\text{s}$ , nonlinear)  
 $t$  = time (s)

The boundary conditions needed to solve Equation 3 are then obtained by first calculating the equilibrium moisture content at 50 % RH using the 1-cm sample series (desorption isotherms). The equilibrium water content of the sample can be calculated from Equation 4.

**Equation 4.** 
$$w_{eq} = \phi - \frac{\Delta M_{eq}}{V}$$

Where:  $w_{eq}$  = Equilibrium volumetric water content at 50 % RH ( $\text{cm}^3/\text{cm}^3$ )  
 $\Phi$  = Porosity ( $\text{cm}^3/\text{cm}^3$ ) (volumetric water content at saturation)  
 $\Delta M_{eq}$  = Mass of water lost under 50 % RH equilibrium conditions (g,  $\text{cm}^3$ )  
 $V$  = Volume of the sample ( $\text{cm}^3$ )

Using results calculated from the above equations, simulations are run to reproduce the average mass loss curves for the 1 and 5 cm samples to determine values for the A and B parameters. Richards' equation is solved using finite element analysis; a 3600 second time step is used for time discretization. Parameter optimization is accomplished by minimizing the difference between the experimental and numerical area under the mass loss curves for the 1 and 5 cm samples.

The first simulations emphasized were performed to estimate the exchange coefficient  $h_w$ , which is important in the first few hours of the drying. See equation 5.

**Equation 5.** 
$$v_n = h_w(w - w_{eq})$$

Where:  $v_n$  = Normal flux imposed at  $X=0$  and  $X=L$   
 $h_w$  = Exchange coefficient (important to the first few hours of drying)  
 $w$  = Volumetric water content ( $\text{cm}^3/\text{cm}^3$ )  
 $V$  = Volume of the sample ( $\text{cm}^3$ )  
 $w_{eq}$  = Equilibrium volumetric water content at 50 % RH ( $\text{cm}^3/\text{cm}^3$ )

Additional simulations to reproduce the average mass loss curves for the 1 and 5 cm samples provide values for the A parameter in equation 2 for the SRS Saltstone vault concrete sample.<sup>7</sup>

### 3.3 Adsorption – Desorption Isotherm Test

The objective of this test is to determine equilibrium water content of cementitious materials over a range of relative humidities using adsorption - desorption isotherms. These equilibrium water content data are used in the Richards' equation as described in the previous section to estimate boundary conditions at the soil / concrete interface for unsaturated

<sup>7</sup> Analysis of numerous mature concrete samples indicates that the A parameter is in the range of  $E-14 \text{ m}^2/\text{s}$  and that values for the A parameter increased as a function of the water to cement ratio.

conditions when performing long-term durability analyses. The data will also be useful to estimate the Van Genuchten parameters and the capillary characteristics of the material. The procedure for this test is described in Attachment 2.

### **3.4 Concrete Immersion Test**

The objective of this test is to evaluate the response of concrete to corrosive solutions that represent potential environmental solutions or leachates. The test method provided in Attachment 2 includes sampling and analysis of the cementitious material for penetrated ionic species that are acid soluble.

The results of the immersion tests will be used to validate the calculated transport properties determined by the STADIUM<sup>®</sup> code using parameters summarized above.

### **3.5 Pore Solution Extraction Test**

The objective of the pore solution extraction test is to provide compositions for saltstone and saltstone vault concrete pore solutions in order to estimate a composition of potentially corrosive leachate generated by exposure of the vault concrete to saltstone and to saltstone leachate produced by contact with infiltrating water. The pore solution extraction procedure and apparatus is illustrated in Attachment 2 Appendix C. The extraction is typically performed using 50,000 psi (345 MPa) pressure.

## **4.0 REFERENCES**

Burns, H. H. 2008. "Program Plan for the Science and Modeling Tasks in Support of the Z-Area Saltstone Disposal facility Performance Assessment (U)," SRNL-ECP-2008-00001 Rev. 0, Washington Savannah River Company, Savannah River National Laboratory, Savannah River Site, Aiken, SC 29808.

WSRC Contract No. SIMCORD08009, Order No. AC48992N, "Saltstone Vault Sulfate Attack and Saltstone Durability," Washington Savannah River Company, Savannah River National Laboratory, Savannah River Site, Aiken, SC 29808.

**5.0 ATTACHMENT 1**

**Summary of Subcontract SIMCORD08009  
Order No. AC 48992N Work Requirements**

**BLANK PAGE**



**SUBCONTRACT SIMCORD08009**  
**Order No. AC 48992N WORK REQUIREMENTS**

**Task Descriptions**

**Task 1. Preliminary estimate of service life.**

Predict degradation using literature data for concrete properties using mixes similar to the WSRC mixes or actual data supplied by SRNL for exposure to up to three (3) different corrodent solutions as specified by the STR at a later date.

Use STADIUM<sup>®</sup> and/or other modeling capabilities to predict the depth of penetration (diffusion front) of corrodents, including sulfate, aluminate, chloride, sodium, etc., in 2 different concretes exposed to 3 different solutions for extended time (up to 10,000 years):

- a. Estimates values for the important parameters from data provided by SRNL and by analogy to similar materials previously tested by SIMCO, Inc.
- b. Run the STADIUM<sup>®</sup> code for a rough estimate of depth of penetration.
- c. Estimate service life taking into consideration penetration depth, formation of expansive phases, and consequence of formation of expansive phases including effect of reinforcement and post tensioning steel.
- d. Estimate the effective transport properties (effective permeability, effective diffusivity coefficient, effective porosity, etc.), according to in-house protocol in addition to providing an estimate assuming the concrete is fully degraded behind the advancing front and intact (not degraded) ahead of the front with respect to computing effective transport properties – if the two approaches are different.

**Task 2. Measure relevant properties for SRS mixes.**

Measure parameters for 2 concrete mix designs (on samples cured for 28 and/or 90 days) required to support STADIUM<sup>®</sup> and/or other service life prediction modeling. Up to two (2) different curing times may be requested by the STR.

**Task 3. Estimate for SRS mixes.**

Run STADIUM<sup>®</sup> using data on SRS mixes. Predict depth of penetration of the corrodent species using data generated in 3.1.2 for the 2 concrete mix designs.

Estimate the effective transport properties (effective permeability, effective diffusivity, effective porosity, etc.), according to in-house protocol in addition to providing an estimate assuming the concrete is fully degraded behind the advancing front and intact (not degraded) ahead of the front with respect to computing effective transport properties – if the two approaches are different.

**Task 5. Confirm short term predictions.**

Expose samples for 2 concrete mix designs to up to three (3) different corrodent solutions to support calculated depth of penetration and service life predictions. The exact number of corrodent solutions and the compositions of those solutions will be specified by the STR at a later date.

Analyze samples for relevant data after exposure for 4 months to compare with model predictions. (A request may be made to continue testing to obtain additional data points.) Monitor volumetric changes due to sulfate reactions with the two different concretes. The corrodent solutions will contain at a minimum sulfate, aluminate, chloride, and sodium.

**Task 5. Provide approach and methodology.**

The SIMCO, Inc. proposal will document the approach and methodology, identify information and testing required, identify the number of samples and sample geometry required, recommend laboratory prepared samples or actual samples (Vault 4) or test samples (Vault 2), and include a cost for preparing samples from materials supplied by SRNL. In the event that certain test methods for quantifying advancing fronts of both sulfate (sulfur) and aluminate (aluminum) in concrete (which already contain significant concentrations of S and Al) are determined to involve the use of radio tracers, a joint work scope with SRNL should also be prepared for the proposal.

**Task 6. Estimate the physical effects of sulfate/aluminate and other corrodents of concern exposure.**

Estimate evolution in permeability, diffusivities, and porosity of the 2 SRS concrete mix designs as a function of exposure to each of the three corrodent solutions, as a result of physical/structural damage (e.g. cracking, spalling) to the extent possible with existing capabilities.

**Task 7. Provide approach and methodology.**

Provide a description of the model methodology including how changes in diffusivity, porosity, water diffusivity are determined. Provide description of test methods.

**Task 8. Final Report.**

A draft final report is due on August 15, 2008.

A final reviewed and accepted report is due on September 30, 2008.

Data and modeling runs performed after September 30, 2008 will be submitted in Revisions of the final report within one month after being generated.

**6.0 ATTACHMENT 2**

**Test Methods for Characterizing Transport Properties of Concrete to  
Support the STADIUM<sup>®</sup> Service Life Prediction Code**

**SIMCO Technologies, Inc.  
SUBCONTRACT SIMCORD08009  
Order No. AC 48992N TASK 5**

**BLANK PAGE**



**SIMCO**  
Technologies inc.

Washington Savannah River Company

Subcontract no. AC48992N

Report  
Task 5 - Methodology

July 2008

Prepared by:

SIMCO Technologies Inc.  
203-1400 Boul. du Parc Technologique  
Quebec QC G1P 4R7  
Canada  
(418) 656-0266 tel | (418) 656-6083 fax

**LIMITED LIABILITY STATEMENT:** THIS REPORT IS FOR THE EXCLUSIVE USE OF SIMCO'S CLIENT AND IS PROVIDED ON AN "AS IS" BASIS WITH NO WARRANTIES, IMPLIED OR EXPRESSED, INCLUDING, BUT NOT LIMITED TO, WARRANTIES OF MERCHANTABILITY AND FITNESS FOR A PARTICULAR PURPOSE, WITH RESPECT TO THE SERVICES PROVIDED. SIMCO ASSUMES NO LIABILITY TO ANY PARTY FOR ANY LOSS, EXPENSE OR DAMAGE OCCASIONED BY THE USE OF THIS REPORT. ONLY THE CLIENT IS AUTHORIZED TO COPY OR DISTRIBUTE THIS REPORT AND THEN ONLY IN ITS ENTIRETY. THE ANALYSIS, RESULTS AND RECOMMENDATIONS CONTAINED IN THIS REPORT REFLECT THE CONDITION OF THE SAMPLES TESTED EXCLUSIVELY, WHICH WERE MANUFACTURED FROM MATERIALS PROVIDED TO SIMCO. BY THE CLIENT OR BY THIRD PARTIES. THE REPORT'S OBSERVATIONS AND TEST RESULTS ARE RELEVANT ONLY TO THE SAMPLES TESTED AND ARE BASED ON IDENTICAL TESTING CONDITIONS. FURTHERMORE, THIS REPORT IS INTENDED FOR THE USE OF INDIVIDUALS WHO ARE COMPETENT TO EVALUATE THE SIGNIFICANCE AND LIMITATIONS OF ITS CONTENT AND RECOMMENDATIONS AND WHO ACCEPT RESPONSIBILITY FOR THE APPLICATION OF THE MATERIAL IT CONTAINS.

THE STADIUM<sup>®</sup> MODEL IS A HELPFUL TOOL TO PREDICT THE FUTURE CONDITIONS OF CONCRETE MATERIALS. HOWEVER, ALL DURABILITY-MODELING PARAMETERS HAVE A STATISTICAL RANGE OF ACCEPTABLE RESULTS. THE MODELING USED IN THIS REPORT USES MEAN LABORATORY- OR FIELD-DETERMINED SINGLE VALUES AS INPUT PARAMETERS. THIS PROVIDES A SINGLE RESULT, WHICH PROVIDES A SIMPLE ANALYSIS EVALUATING CORROSION PROTECTION OPTIONS. PREVIOUS CONDITIONS ARE ASSUMED TO CARRY FORWARD IN THE PREDICTION MODEL; THERE ARE NO ASSURANCES THAT THE STRUCTURE WILL BE EXPOSED TO A SIMILAR ENVIRONMENT AS IN THE PAST.

## TABLE OF CONTENTS

<b>1</b>	<b>Objective .....</b>	<b>7</b>
<b>2</b>	<b>Migration test for ionic transport properties of cementitious materials .....</b>	<b>7</b>
2.1	Scope .....	7
2.2	Summary of Test Method .....	7
2.3	Significance and use .....	7
2.4	Apparatus and test cells .....	8
2.5	Reagents and materials .....	8
2.6	Test specimens .....	8
2.7	Specimen Conditioning .....	9
2.8	Test Procedure .....	9
2.9	Report .....	11
2.10	Analysis .....	11
<b>3</b>	<b>Test Procedure for Moisture Transport Coefficient of Concrete by Drying .....</b>	<b>12</b>
3.1	Scope .....	12
3.2	Significance and Use .....	12
3.3	Apparatus .....	12
3.4	Sealing/Coating Materials .....	13
3.5	Test Specimens .....	13
3.6	Procedure .....	14
3.7	Report .....	14
3.8	Analysis .....	15
<b>4</b>	<b>Test Procedure for Adsorption-Desorption Isotherms of Cementitious Materials ..</b>	<b>16</b>
4.1	Scope .....	16
4.2	Summary of Test Method .....	16
4.3	Significance and Use .....	16
4.4	Apparatus and Test Cells .....	16
4.5	Reagents and Materials .....	17
4.6	Test Specimens .....	17
4.7	Setup preparation for each box .....	18
4.8	Procedure for desorption isotherms .....	18
4.9	Procedure for adsorption isotherms .....	19
4.10	Report .....	20
<b>5</b>	<b>Test Procedure for Concrete specimens immersions in different ionic solutions .....</b>	<b>20</b>
5.1	Scope .....	20
5.2	Summary of Test Method .....	21
5.3	Significance and Use .....	21
5.4	Apparatus .....	21
5.5	Reagents and Materials .....	22
5.6	Test Specimens .....	22
5.7	Procedure – exposure simulation .....	22

5.8 Procedure – sampling of pulverized layer .....	23
5.9 Procedure – acid extraction .....	23
5.10 Report .....	24
Appendix A – Assembly of Migration Cells.....	28
Appendix B – Making Solutions for Migration test.....	30
Appendix C – Accompanying Specimen for Pore Solution Extraction .....	32
Appendix D – Recent advances in the determination of ionic diffusion coefficients using migration test results .....	
Appendix E – Determination of the water diffusivity of concrete using drying/absorption test results.....	



## **Objective**

This report on Task 5 presents the methodologies used for experimental tests and durability model simulations. Experimental tests cover the evaluation of the transport properties of concrete and the exposure conditions required to make aggressive species solutions. In this project, the durability model that will be used is STADIUM<sup>®</sup>.

When the transport properties parameters of cementitious materials are determined, durability model simulations of different exposure conditions are compared to experimental data for validation of the calculated parameters.

The present report is divided as follow:

- Section 2 presents the migration test;
- Section 3 details the drying-wetting test;
- Section 4 describes the adsorption-desorption isotherms test;
- Section 5 describes the test for obtaining exposure conditions.

## **Migration Test for Ionic Transport Properties of Cementitious Materials**

### ***Scope***

This test method covers an experimental procedure used to evaluate the diffusion coefficient of ionic species in cementitious materials. This test method is a modified version of the AASHTO T277 and ASTM C1202 -97 standard test procedures.

### ***Summary of Test Method***

The test method consists in monitoring the intensity of electrical current passed through a cylindrical test specimen during a 10-day testing period. An appropriate DC potential is maintained constant across the specimen by an electrical power supply. The upstream cell is filled with a chloride-containing electrolytic solution and connected to the negative electrode, while the downstream cell is filled with a base solution and connected to the positive electrode. If desired, chloride ion penetration through the specimen can be monitored by periodically analyzing the chloride content in the downstream cell.

### ***Significance and use***

The ionic diffusion coefficients are the main transport parameters. These coefficients must be evaluated in order to perform a numerical simulation to estimate the service life of a concrete structure. The numerical results are the recorded current intensities during testing. They provide the information required to evaluate the ionic diffusion coefficients.

### ***Apparatus and test cells***

Assembly of migration cells [See Appendix A]

Constant voltage power supply - output: 0-30V DC; capacity: 0-2A

Digital voltmeter: measurement of DC potentials in the 0-24 volts range and current intensity, to 0.1 mA accuracy in the 0-200 mA range and 0.01A accuracy in the 0.2-1 A range.

Electrically conductive wires to connect the power supply output to the electrodes through jacks attached to the test cells. The electrical resistance of each wire should be less than 0.01 Ohm.

Measuring probes for insertion through the small holes in the cells to measure potential difference across the specimen. One end of the probe connects to the jack on the voltmeter.

Vacuum saturation apparatus (vacuum pump, container, pressure gauge, etc.)

Specimen sizing apparatus (rulers)

Balance (repeatability: 0.01g)

Funnel and containers (made of chemical-resistant materials)

### Reagents and materials

Aqueous solution of 0.5M sodium chloride (NaCl) mixed with 0.3M sodium hydroxide (NaOH) [See Appendix B]

Aqueous solution of 0.3 M Sodium Hydroxide (NaOH) [See Appendix B]

Sealant: waterproof silicon sealant is recommended.

Distilled or deionised water for solution preparation.

### ***Test specimens***

Cylindrical specimens are required for the test. It is recommended to test at least two samples per concrete mixture. Specimens should be 96-102mm (i.e., approximately 4-in.) in diameter. Concrete specimens should be  $50 \pm 1$  mm (4-in.) thick. Mortar specimens should be 35-50 mm thick. Sample preparation and selection depend on the purpose of the test. Test specimens may be obtained from laboratory cast cylinders or cores extracted from existing structures. All specimens should be properly identified prior to testing. A companion specimen is needed for pore extraction. A further sample is needed for porosity measurement according to ASTM standard 642. These supplementary tests provide data for purposes of migration test analysis. For relevant results, these additional samples should have identical histories (curing, exposure conditions, and storage conditions) to the testing samples.

### *Specimen Conditioning*

Test specimens should be vacuum saturated with 0.3M NaOH for approximately 18 hours following the procedure described in ASTM 1202-97: 9. A companion sample is saturated in the same container to be used for pore solution extraction (see Appendix C). The saturation procedure is summarized as follows: immerse the specimens in the 0.3M NaOH solution contained in the vacuum container. Turn on the vacuum pump. When the pressure gauge shows maximum vacuum pressure (less than 1 mm Hg -133 Pa), keep the pump running for about 2 hours. With all valves closed, turn off the pump and maintain vacuum conditions for 18 hours. Open the air valve to release the pressure.

### *Test Procedure*

Dry the surfaces of the vacuum-saturated specimens with a clean cotton cloth or soft tissue. Measure the dimensions of each specimen. Diameter and thickness should be measured to a precision of at least 0.1 mm or better. Each parameter is determined by the average of 2 measurements from different positions. Weigh the surface-dried specimen to a precision of 0.1 g.

Seal and mount each specimen onto the two connecting rings (See Appendix A) by using silicone and completely coat all side surfaces with silicon (about 2-3 mm thick, Figure 1).

Place the specimens in a well-ventilated area and cover the exposed surfaces with wet paper for about 2 hours until the silicone is almost dry and strong enough for handling.

Remove any surplus silicone from the inner surface of the specimen along the ring edges to obtain maximum exposure surface. Make sure to minimize contamination of the exposed surfaces by silicone (Figure 1).

Measure the diameter of the specimen's actual exposure area using two measurements at different positions across the radial section. This diameter should be approximately the same as the diameter of the ring mouth.

Mount the specimen and the two rings onto the two cells (Figure 2). To avoid leakage, apply vacuum grease where the ring assembly comes into contact with the cells. Securely tighten the bolts that hold the two cells together. Cells should be alternatively filled with water to verify that there is no leakage. After this control step, empty the water from the cells and remove water surplus with a soft tissue.

Fill the downstream cell with 0.3M NaOH solution.

Fill the upstream cell with 0.5M NaCl + 0.3M NaOH solution.

Place the setups in their testing sites then connect all the electrodes on the upstream cells to the negative output of the electricity power supply. Connect all the electrodes on the downstream cells to the positive output of the power supply (Figure 2).

Turn on the power supply. Adjust the potential output to obtain a potential difference of  $10 \pm 0.2$  V across all specimens. Potential difference across the specimen is measured with two bent probes. Connect the two probes into the voltmeter (plug in the jacks), set the proper range for the voltmeter (e.g., 0-20V), insert the probes into

the cells through the holes in the cells and place each end probe in contact with the surface of the specimen that is immersed in the solution. Wait for the reading to stabilize, then record the voltmeter reading (*Note:* the potential difference across the specimen is 2-3 volts lower than the output as shown on the power supply or measured from the two electrodes of the cells).  
Measure the current passing through each specimen.

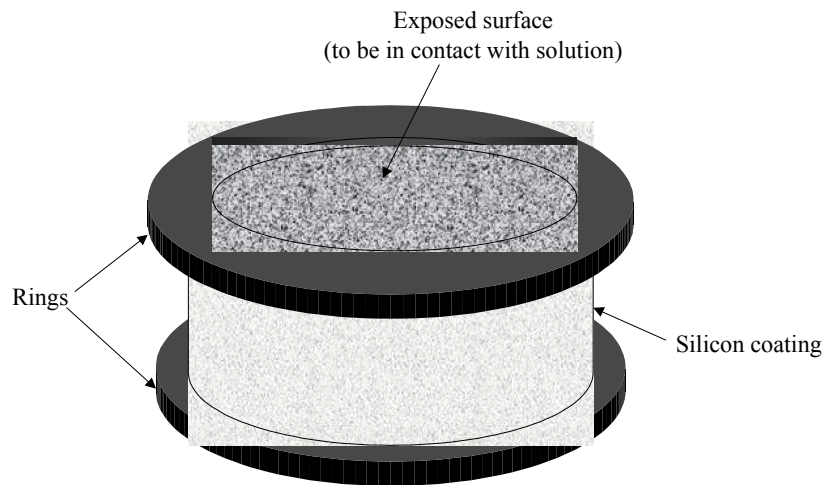


**Figure 1 - Test specimen sealed and mounted onto the two rings and coated with silicone**

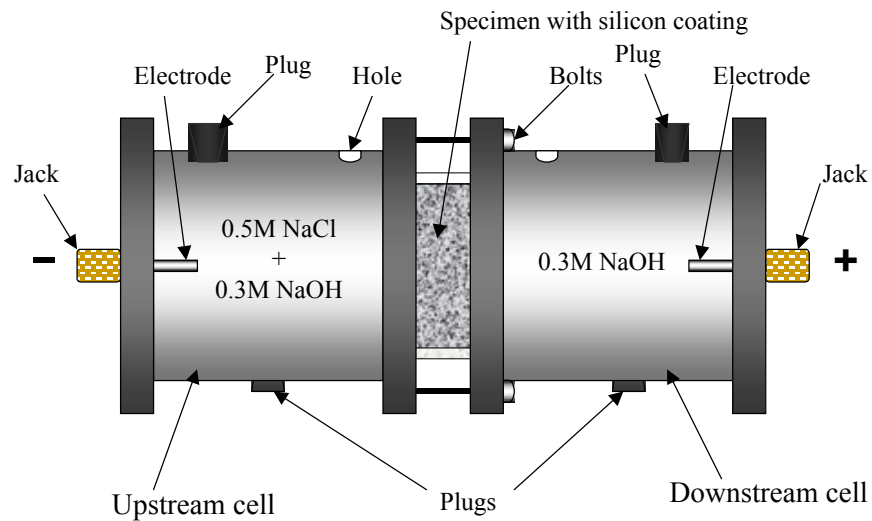


**Figure 2 - Setup of migration test**

If the current is below 100 mA, the potential level has been properly set. Record the initial readings of the current intensity (to 0.1 mA accuracy) and the potential across the specimen (to 0.1V accuracy). Also, record the date and time.

If the current is above 100 mA, decrease the potential output to bring the current down to the proper level. Record the initial current and potential measurements as well as the time of measuring.

If the initial current under a low potential (e.g., 6V) is higher than 100 mA, stop that test. This indicates a very porous material.

A power supply can run a set of tests if they share the same potential output. The maximum number of tests depends on the supply output power and total current intensity. When tests share the same power supply, set the supply current control to maximum range to ensure a sufficient power output under the desired constant potential. During testing, both current intensity passing through the specimen and the potential difference across the specimen might vary within a certain range, even though electrical output remains stable and constant.

During the first day of testing, take measurements of the current intensity passing through each specimen and the potential difference across each specimen at 0, and 4 hours of duration respectively. Record the time for each measurement.

After the first day, take measurements of the current passing through each specimen and the potential difference across each specimen at 24-hour time intervals for 10 days. Record the time for each of these measurements.

### ***Report***

Report the following, if known:

Information on the specimens: origin (e.g., mixture ID and curing age of the concrete tested), dimensions, mass before and after vacuum saturation, and effective test exposure area (in diameter) for both upstream and downstream sides.

Test results for companion samples: porosity and pore solution analysis.

Experimental record sheet including test specimen IDs, test conditions, date and time of each measurement, and all readings of potential across the specimens and currents passed through the specimens for the entire testing period.

Any abnormal phenomenon observed in the test such as changes in solution color, solution precipitation, excessive gas evolution from the electrodes, unusual odors, accidents or problems concerning the electricity supply, etc.

## **Moisture Transport Coefficients**

The analysis consists of reproducing the current with the ionic transport model STADIUM<sup>®</sup>. The tortuosity of the material is adjusted until the sum of the ionic fluxes corresponds to the measured current. A detailed description of the analysis is given in Appendix D, Test Procedure for Moisture Transport Coefficient of Concrete by Drying

### ***Scope***

This test method is used to determine the drying rate of Portland cement concrete by measuring the mass loss due to evaporation and moisture transport in specimens exposed to constant temperature and relative humidity.

### ***Significance and Use***

Drying behaviour reflects the mass transport properties of concrete to a certain extent, based on many factors such as: (a) concrete mixture proportions; (b) presence of chemical admixtures and supplementary cementitious materials; (c) composition and physical characteristics of the cementitious components and aggregates; (d) entrained air content; (e) curing type and duration; (f) degree of hydration and age; (g) presence of microcracking; (h) presence of surface treatments such as sealers or form oil; and (i) placement method, including consolidation and finishing. Concrete drying is also strongly affected by the moisture condition of the concrete at the time of testing and the controlled temperature and relative humidity environment.

### ***Apparatus***

**Drying chamber:** The test is performed in a walk-in environmental testing chamber. The chamber should be sufficiently spacious to contain all test specimens and weighing instruments. The operator should be able to take measurements within the chamber. Air in the chamber should be maintained at  $23\pm 2^{\circ}\text{C}$  and  $50\pm 4\%$  relative humidity (RH). Air-flow rate past the specimens should meet ASTM C157: 5.4 Standard specifications.

**Hygrometer:** During testing, 2-3 hygrometers should be placed near the specimens to monitor local relative humidities. Digital hygrometers are recommended.

**Balance:** The balance for weighing the specimens should have a capacity of  $\geq 1500\text{g}$  and a repeatability of  $\leq 0.01\text{g}$ . It should be mounted on a proper support (Figure 3) within the drying chamber.

**Device for weighing specimens in water:** A device should be devised for the operator to weigh the specimens in water (Figure 3).

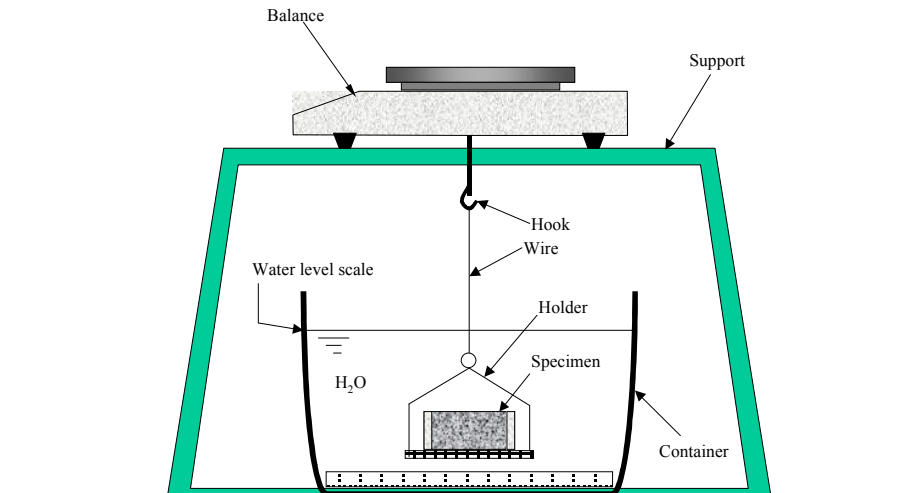


**Figure 3 – Balance and device for weighing specimens in water within the drying chamber**

### *Sealing/Coating Materials*

Epoxy: Epoxy that can be used with concrete and that produce impermeable material to seal and coat specimens.

Duct tape: Duct tape is used for coating and sealing.

### *Test Specimens*

Test specimens should be fully hydrated concrete (e.g., >3 months curing) to prevent detectable structural changes during testing.

Test specimens should be cylindrical, either cut from cast cylinders or extracted from cores. A typical cylindrical specimen should be  $100 \pm 2$  mm (i.e. 4 inches) in diameter. All specimens from a single material should have equal diameters.

Two  $11 \pm 1$ -mm and  $50 \pm 2$ -mm thick discs should be cut for each material tested (concrete mixture).

Three  $11 \pm 1$ -mm and three  $50 \pm 2$ -mm specimens should be prepared for each material tested.

Cut specimens should be kept constantly moist until testing, and should be coated with epoxy after weighing in air and water (see Section 3.6).

Note: Since other tests (e.g., porosity measurements) are usually performed along with the drying test, specimens should be cut from the same concrete cylinder.

### ***Procedure***

Measure the dimensions of each cut specimen: take two diameter and two thickness measurements with a precision of 0.1 mm.

In the drying chamber, weigh each cut specimen in water using the balance and setup illustrated in Figure 3.

Dry the surfaces of each specimen with clean, dry tissue and weigh it in air using the balance in the drying chamber.

Apply tapes to both flat surfaces and dry the curved surface further with air pressure.

Coat the curved surface of each specimen with epoxy (Figure 4).

Once the epoxy coating has hardened, remove the protective tapes to expose the flat surfaces having the same diameter as the specimen (Figure 4).

Transfer the coated specimens to the drying chamber. Weigh each coated specimen in air using the above-described balance (to obtain initial weights for the drying test), then mount them on the support in the chamber for drying (Figure 5).

Weigh each specimen according to the schedule below:

- Day 1: 3 measurements at 0-, 1- and 6-hour intervals.
- Day 2 to Day 7: one measurement every 24 hours.
- Day 8 and later: three measurements per week.

Stop weighing when the 10-mm thick specimen reaches equilibrium mass change: five successive mass change determinations are constant within  $\pm 0.005\%$  of specimen mean value. At this point, stop testing on all specimens.

After the final drying measurements, transfer all the specimens (10 mm-thick and 50 mm-thick specimens) into a container with enough water in it to submerge all the specimens for “absorption” test.

Take measurements of surface-dried coated specimen mass using the balance in the drying room according to the following schedule:

- 7 measurements (including final drying weighing) at least 24 hours apart during days 1 to 7. Tolerance on time measurement should be within 3 hours. The actual time of each measurement should be recorded to within 5 minutes.
- 3 measurements per week at least 48 hours apart after day 8.

Absorption process can be terminated when constant weight is observed for both of the 1cm-thick and 5cm-thick specimens (i.e. the mass change during a 3-day interval is within  $\pm 1\%$  of the total mass gain), which indicates fully re-saturation of the specimens.

### ***Report***

Report the following:

Date when specimen was cast or extracted.

Concrete mixture or material reference number and all other relevant information (cement type, cure duration, w/c ratio, etc.).



For each tested specimen, provide a table including complete experimental records and all dimensions measured.

Plot experimental measurements against testing time.

Plot the remaining water content of each tested specimen against testing time once material porosity has been determined. Remaining water content is calculated by the following procedure: volume of specimen (cm<sup>3</sup>) = Weight in air (g) – Weight in water (g); remaining water content (%) = [(Porosity (%) x Volume (cm<sup>3</sup>)/100 – cumulative mass loss (g)]/Volume (cm<sup>3</sup>) x 100.

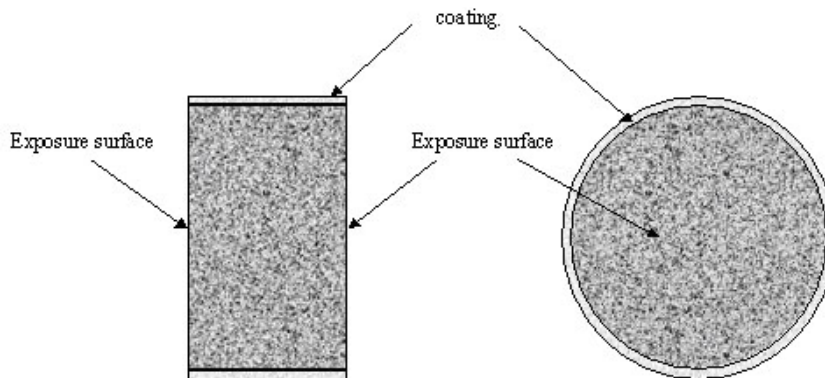


**Figure 4 – Coated curved surface of the test specimen (cutaway view on the left, top view on the right)**

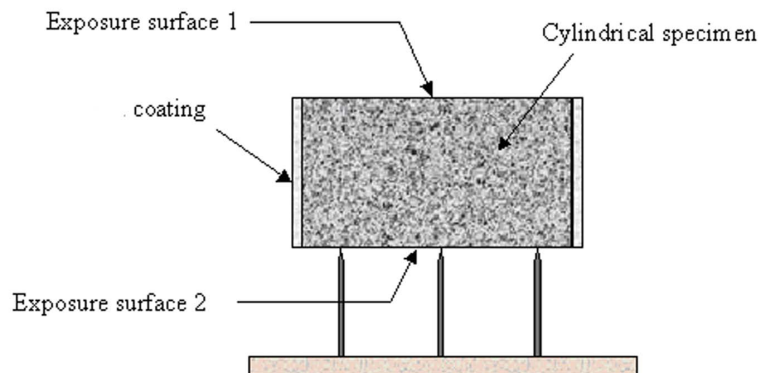


**Figure 5 – Coated specimen in the uniaxial drying test (cut away view)**

### *Analysis*

The analysis of the mass loss curves using Richards' equation allows estimating the nonlinear water diffusivity, expressed as:  $D_w = Ae^{Bw}$ . A detailed description of the analysis procedure is given in Appendix E.

## **Test Procedure for Adsorption-Desorption Isotherms of Cementitious Materials**

### ***Scope***

This test method covers the measurement of the equilibrium water content of cementitious materials exposed to a specific relative humidity environment. This test method provides both desorption and adsorption isotherms.

### ***Summary of Test Method***

This test method consists of monitoring the mass of cementitious materials in a constant relative humidity environment and in a constant temperature until materials reach moisture equilibrium. Pre-conditioning procedures for obtaining initial moisture conditions of the specimens depend on desorption or adsorption isotherms tests, which issue will be chosen. The different relative humidity environments are controlled in vapor resistant boxes by using supersaturated salt solutions.

### ***Significance and Use***

Isotherms give the equilibrium relationship between relative humidity and water content of the tested material.

The shape of the isotherms depends on many factors including: (a) concrete mixture proportions, (b) presence of chemical admixtures and supplementary cementitious materials, (c) composition and physical characteristics of the cementitious component and aggregates, (d) entrained air content, (e) type and duration of curing, (f) degree of hydration or age, (g) presence of microcracks, (h) presence of surface treatments such as sealers or form oil and (i) placement method including consolidation and finishing. Isotherms are also affected by the initial moisture condition and temperature of the concrete at the time of testing.

### ***Apparatus and Test Cells***

Testing room – The test is performed in a walk-in environmental testing room. Temperature in the room should be maintained at  $23 \pm 2^\circ\text{C}$ .

Drying Oven - The oven shall be maintained at a temperature of  $105 \pm 5^\circ\text{C}$ .

Controlled relative humidity boxes - Sixteen vapor-resistant boxes are used, one for each relative humidity condition and for each initial moisture condition (desorption or adsorption isotherms). The size of the boxes should be suitable for maintaining specified relative humidity when a set of soaked specimens are introduced inside.

Pan – Sixteen pans should be resistant against salts and remain at the bottom of the box.

Hygrometers - Relative humidity and temperature in the boxes must be measured at regular interval to control the efficiency of supersaturated salt solutions.

Balance - The balance must have a sufficient capacity for the tested specimens and accurate to at least  $\pm 0.001\text{g}$ .

Device for weighing specimens in water - Device for weighing specimens in water: A device should be devised for the operator to weigh the specimens in water (Figure 3).

Towel - Used to wipe out water from the surface of the specimens.

Containers – Containers should be suitable to immerse all specimens during conditioning and be vapor-resistant for storing specimens before adsorption test.

### ***Reagents and Materials***

LiCl. - Supersaturated solution that maintains relative humidity at 11.3% in room at  $23 \pm 2^\circ\text{C}$ .

MgCl<sub>2</sub> - Supersaturated solution that maintains relative humidity at 33.1% in room at  $23 \pm 2^\circ\text{C}$ .

MgNO<sub>3</sub> - Supersaturated solution that maintains relative humidity at 54.4% in room at  $23 \pm 2^\circ\text{C}$ .

NaCl. - Supersaturated solution that maintains relative humidity at 75.5% in room at  $23 \pm 2^\circ\text{C}$ .

KCl - Supersaturated solution that maintains relative humidity at 85.5% in room at  $23 \pm 2^\circ\text{C}$ .

BaCl<sub>2</sub> - Supersaturated solution that maintains relative humidity at 91% in room at  $23 \pm 2^\circ\text{C}$ .

KNO<sub>3</sub> - Supersaturated solution that maintains relative humidity at 94.6% in room at  $23 \pm 2^\circ\text{C}$ .

K<sub>2</sub>SO<sub>4</sub> - Supersaturated solution that maintains relative humidity at 97.3% in room at  $23 \pm 2^\circ\text{C}$ .

Lime - to decrease the concentration of carbon dioxide in the sealed environment

Water – Temperature of water should be kept at  $23 \pm 2^\circ\text{C}$  to determine apparent mass of specimens. Tap water is suitable for the adsorption test.

### ***Test Specimens***

Test specimens should be fully hydrated concrete (e.g., >3 months curing) to prevent microstructural changes during testing.

Specimens should have high specific surface area and representative volume. This obtained by sawing several thin slices from representative cylinder.

For normalweight concrete, a practical specimen should be a  $100 \pm 2$  mm diameter disc with a thickness of  $10 \pm 1$  mm. Useful specimen of cement paste may be as thin as 1 to 2 mm with a section area about 20 – 25 cm<sup>2</sup>.

Following previous design, five specimens are required for each relative humidity condition and for each initial moisture condition (desorption and adsorption).

The test specimens should be kept constantly moist during specimen preparation.

### ***Setup Preparation for Each Box***

The preparation of the boxes should be done in the testing room.

The box should be able to contain five concrete specimens as described in the previous section; for this specific project the box size should be 200 by 300 mm and 270 mm in height. The pan should be 125 by 205 mm and 85 mm in height.

Spread a layer of 1 cm of dry salt in the pan. Add water while mixing to obtain a supersaturated solution. Presence of visible crystals in the solution provides acceptable evidence of saturation. Then place the pan at the bottom of the box.

Install a rigid plastic grid on the pan to support specimens. Place a well spaced grid at mid-height of slice which will allow maintaining the elevation of the specimen and provides sufficient clearance (at least 10 mm) between specimens.

Lime should be added in the box to decrease the concentration of carbon dioxide in the sealed environment.

Install carefully the hygrometer on one side of the box. The information given by the hygrometer should be easily accessible (visible for reading) to the operator.

Close the box and wait for equilibrium in the sealed environment (box) to be reached before storing specimens (usually takes one day).

### ***Procedure for Desorption Isotherms***

Immerse the specimen in water at approximately  $23 \pm 2^\circ\text{C}$  until two successive values show an increase in mass of the surface-dried sample less than 0.5% of the larger value at intervals of 24h. Surface-dry the specimen by removing the moisture with a towel and determine the mass.

Determine the immersed apparent mass of each specimen by weighing it in water using the balance.

Inside the testing room, place a set of five soaked surface-dried specimens previously weighed in the same box for each relative humidity, then record the date and time at the beginning of the desorption isotherm test.

Record the specimen's mass using the balance in the testing room according to the following schedule:

- 1 measurement every four weeks until two successive mass determinations show a variation within  $\pm 0.5\%$  of the total mass loss at this time.
- Then take 1 measurement every two weeks.

Stop desorption isotherm test when the specimen reaches equilibrium mass change: five successive mass determinations are constant within  $\pm 0.5\%$  of the total mass loss at this time.

When equilibrium is reached, oven-dry the samples at a temperature of 100 to  $110^\circ\text{C}$  until the difference between any two successive values of the mass, at least 24 hours apart, is less than 0.5% of the lowest value obtained. The measurements of the specimen's mass must be determined after cooling in dry air at a temperature of  $23 \pm 2^\circ\text{C}$ . Record the oven-dried mass.

***Procedure for adsorption isotherms***

Immerse the specimen in water at  $23 \pm 2^\circ\text{C}$  until two successive values at intervals of 24h show an increase in mass of the surface-dried sample less than 0.5 % of the larger value. Surface-dry the specimen by removing the moisture with a towel and determine the mass.

Determine the immersed apparent mass of each specimen by weighing it in water using the balance and set-up indoor testing room. Then, remove the surface moisture with a towel and determine the soaked surface-dried mass of each specimen by weighing it in the air.

Condition the specimens in a cabinet at  $40 \pm 2^\circ\text{C}$  with silica gel until their mass are within  $\pm 0.5\%$  of the expected oven-dried mass which is estimated by the following equations:

$$M = \frac{B}{1 + \frac{Ab}{100}}$$

• where:

B = mass of soaked surface-dry specimen in air (g).

M = expected mass of oven-dry specimen (g).

Ab = absorption after immersion, according to ASTM C642 (%).

Store the dried specimens in a vapour resistant box for at least 15 days before the start of adsorption isotherm tests and then record the relative humidity inside the box.

Inside the testing room, place a set of five dried specimens previously weighed, in the same box for each relative humidity, then record the date and time as the adsorption isotherm test begins.

Take measurements of the specimen mass using the balance in the testing room according to the following schedule:

- 1 measurement every four weeks until two successive mass determinations show a mass variation within  $\pm 0.5\%$  of the total mass loss at this time.
- Then take 1 measurement every two weeks.

Stop the adsorption isotherm test when the specimen reaches equilibrium mass change: five successive mass change determinations are constant within  $\pm 0.5\%$  of the total mass gain at this time.

When equilibrium is reached, oven-dry the samples at a temperature of 100 to  $110^\circ\text{C}$  until the difference between any two successive values of the mass, 24 hours apart, is less than 0.5% of the lowest value obtained. The measurements of specimen's mass must be determined after cooling it in dry air at a temperature of  $23 \pm 2^\circ\text{C}$ . Record this mass as oven-dried mass.

## ***Report***

Report the following:

Information about the specimens - mixture ID and curing age of the concrete tested and porosity based on ASTM C642 Standard Test Method for Density, Absorption, and Voids in Hardened Concrete measured at the start of the adsorption/desorption test.

Experimental recording sheet that includes the ID of the test specimens, apparent mass in water and the corresponding mass of the surface-dry specimens in the air, the oven-dry mass, the test conditions (temperature and relative humidity), date and time of each measurement, and all the readings of mass during conditioning and adsorption or desorption tests.

Plot the remaining water content at both desorption and adsorption isotherms versus relative humidity. Remaining water content is estimated by the following equations:

- $$V = \frac{B - A}{\rho}$$
- $$w(RH) = 100 \times \frac{C - D}{V}$$

where:

V = volume of uncoated specimen (cm<sup>3</sup>)

A = apparent mass of soaked specimen in water (g)

B = mass of soaked surface-dry specimen in air (g)

C = mass of specimen in moisture equilibrium with specified RH (g)

D = mass of oven-dry specimen (g)

ρ = density of water = 1 g/cm<sup>3</sup>

w(RH) = water content at moisture equilibrium (%)

If needed, the remaining water content can be approximated by the following equations:

- $$w(RH) = W - 100 \times \frac{B - C}{V}$$

where

W = volume of permeable pore space, according to ASTM C642 (%).

## **Test Procedure for Concrete specimens immersions in different ionic solutions**

### ***Scope***

This test method covers the simulation of one or more exposure conditions that could be in direct contact with cementitious materials. This test method covers the sampling and analysis of cementitious materials for penetrated ionic species that are acid soluble. This test method provides information that can be used for validating the calculated transport properties evaluated by the methods presented earlier.

### ***Summary of Test Method***

This test method consists of immersing concrete specimens in a salt solution and evaluating the ions profiles after a certain exposure time. After the specified exposure time, the concrete is pulverized at different depths from the exposed surface. Ionic species, such as chlorides and sulfates, are extracted from each pulverized samples by acid digestion and filtration. The ionic analysis of the filtrate gives the concentration in ions and the content per mass of cementitious material is calculated. With the results, the ion profile is given.

### ***Significance and Use***

This test method covers the concentration determination of ionic species in cementitious materials that are acid soluble.

The experimental results - the concentration in cementitious material of acid soluble ionic species versus penetration depth provides information to validate the transport properties measured on the concrete.

### ***Apparatus***

Use the following apparatus to produce different exposure condition:

Containers - The containers in which the specimens are immersed shall be corrosion resistant such as plastic, glass, or ceramic. Seal the container with a lid so that the solution can not evaporate.

Testing room - The test is performed in a walk-in environmental testing room. Temperature in the room should be maintained at  $23 \pm 2^{\circ}\text{C}$ .

pH-meter

Use the following apparatus for pulverization of the concrete using a drill:

Drilling bit of sufficient diameter to drill and pulverize a representative quantity of concrete.

Brush to remove pulverized material from drilled hole without contamination.

Air compressor to clean sampling tools.

Sample containers capable of maintaining pulverized concrete without any contamination from the outside.

Use the following apparatus for acid extraction of ionic species:

Balance shall be capable of reproducing results within 0.0002 g with an accuracy of  $\pm 0.0002$  g.

250mL Beakers

Stirring bar.

Hot plate – It should be equipped with magnetic stirrer to heat one liter of liquid at  $70^{\circ}\text{C}$ .

Filtration device – It is composed of 250 mL or 500 mL Buchner funnel and filtration flask using suction.

100 mL bottles – Suitable to resist acid liquid in filtration.

### ***Reagents and Materials***

Sealing material - Various brands of commercial epoxy may be used. The product should be impermeable and resistant to the exposure solution. Its use with concrete should be approved by the manufacturer.

De-ionized water - It is used to make the solutions and dilute some reagents.

Salt of interest such as, but not limited to, Sodium Chloride (NaCl), Sodium Hydroxide (NaOH), Sodium Sulfate (Na<sub>2</sub>SO<sub>4</sub>), and Calcium hydroxide (Ca(OH)<sub>2</sub>).

0.1 M HNO<sub>3</sub> acid

### ***Test Specimens***

Normally, two specimens should be prepared for each type of exposure (exposure time and exposure solution).

For normal concrete, the specimen should have a diameter of  $100 \pm 2$  mm and a thickness of  $100 \pm 2$  mm. It can be obtained by sawing a conventional 100 mm diameter concrete cylinder at mid-height. Sawn surface should be used as exposed surface.

Coat the surface of each specimen with sealing material leaving one flat cut surface uncoated as the “exposed surface”.

Unless otherwise directed, place the specimens in a safe place covered with a moist tissue on the uncoated surfaces for 2-3 hours until the coating becomes hardened. Then place the coated specimens into the fog room or immerse them in a container full of water over night.

### ***Procedure – exposure simulation***

Salt shall be dissolved and diluted with distilled or deionized water to obtain specified concentrations.

Mix the exposure solution one day before the start of the immersion, cover, and store at  $23 \pm 2^{\circ}\text{C}$ .

Immerse the coated specimens in storage container and record the date.

Maintain the volume ratio of exposure solution to specimens at 3.5 (solution/specimens).

For concrete specimens with a 100 mm diameter and 100 mm in height (volume 785 cm<sup>3</sup>), to respect the ratio it requires at least 2,750 cm<sup>3</sup> of solution per specimen.

Renew exposure solution every three months for all immersion conditions.



***Procedure – sampling of pulverized layer***

At the specified exposure time, remove two companion specimens from exposure solution and then dry the specimen surfaces using compressed air.

Immediately proceed to the pulverization of the concrete at different depths from the exposed surface.

Clean all sampling tools prior each sampling operation. Sampling tools may be cleaned with compressed air.

Using pulverized bit, drill perpendicular to the concrete surface to a specified depth or a depth sufficient to obtain a representative sample of concrete. Sample of at least 20 grams is representative when the nominal maximum coarse aggregate size is less than 25 mm.

To prevent sample contamination, avoid contact with hands and other sources of perspiration.

Transfer powdered sample into sample container using a spoon or other suitable means.

Take two measurements of the depth from the exposure surface to the layer bottom.

Repeat sampling operation until desired final depth.

Oven-dry pulverized samples at  $105 \pm 5^{\circ}\text{C}$  during at least five hours. Cool samples in dry air at  $23 \pm 2^{\circ}\text{C}$  and store all the material passing the 850- $\mu\text{m}$  [No. 20] sieve in a sealed plastic bag.

***Procedure – acid extraction***

Heat above  $70^{\circ}\text{C}$  0.1 M  $\text{HNO}_3$  acid in a beaker placed on hot plate equipped with magnetic stirrer.

Determine the mass of 5.0000 g of dry sample to the nearest 0.0002 g into a 250 mL beaker.

Slowly add 50 mL of hot 0.1 M  $\text{HNO}_3$  acid and stir with a glass rod, breaking up any lumps of sample.

Cover the beaker with a watch glass and let stand for at least 1 hour.

Filter the sample through a coarse-textured filter paper in a 250 mL or 500 mL Buchner funnel and filtration flask using suction. Rinse the beaker and the filter paper twice with a little de-ionized water. Transfer the filtrate from the flask to a 100 mL bottle and rinse the flask once with de-ionized water. The volume should not exceed 55 mL.

NOTE - It is not necessary to clean all slurry residues in the beaker, nor is it necessary that the filter remove all the fine material. The titration may take place in a solution that contains a small amount of solid matter.

Analyze the ionic concentrations of the filtrate with appropriate technique such as potentiometric titration for chlorides or Ion Chromatography for sulfates.

***Report***

Report the following, if known:

Information about the specimens - mixture ID, mixture composition and curing age of the concrete tested.

Experimental recording sheet that includes the ID of the test specimens, the test conditions, time of exposure, for each pulverized sample, the average depth to the nearest 0.1 mm at mid height of the layer, concentration of ionic species in percent by mass of dry cementitious material to the nearest 0.001%. Calculate percent ionic species by mass of dry cementitious material as follows:

$$C = 100 \times 10^{-3} C_f \times \frac{10^{-3} V}{W}$$

where:

C = percent ionic species by mass of dry cementitious material, %.

C<sub>f</sub> = concentration of ionic species in filtrate, ppm.

W = mass of sample, g.

V = volume of filtrate, mL.

## Appendix A – Assembly of Migration Cells

### *Cells*

The migration test cells consist of two symmetrical chambers made of polymer materials (e.g., methyl methacrylate). Each cell is equipped with an electrode (see below) and an external connector (jack). The volume of each cell should be approximately 3 liters. The mouth of the cell should fit the connecting ring.

### *Connecting Rings*

Two connecting rings are needed for the test setup. The ring should be made of polymer materials and designed to hold the specimen from one side and connected to the cell from the other side. The exposure area should be as large as possible. A typical design for the 4-in. cylindrical specimens is shown in Figure A1.

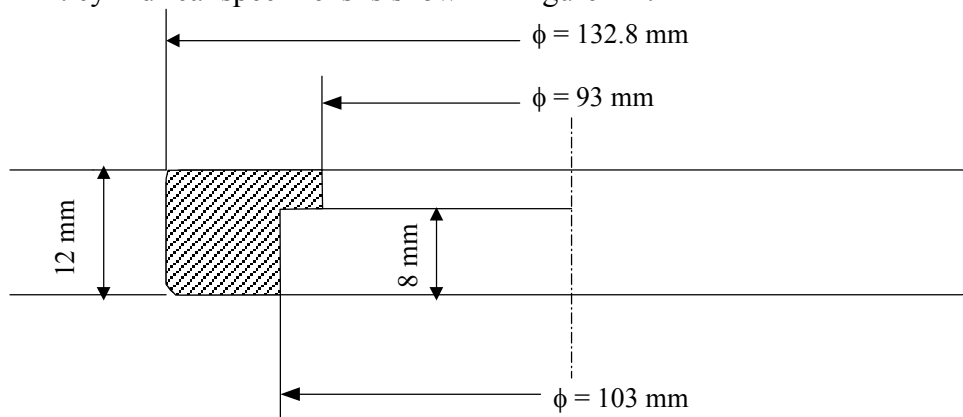


Figure A 1 – Connecting ring for 4-in specimen (96-103 mm)

### *Electrodes*

A rod electrode is installed on each cell. Carbon electrodes should be avoided because they tend to decompose in the electrolytic solution under the application of a DC potential. Electrodes made of titanium or ruthenium oxide with titanium coating are recommended. Each electrode should be securely connected to the external connector by the jack (Figure 2).



**BLANK PAGE**

## Appendix B – Making Solutions for Migration Test

### Solution preparation

The following procedure describes the preparation of the aqueous solutions:

Accurately weigh the salt or base (e.g., NaCl or NaOH) of high purity (>99%) to at least 0.001g accuracy (refer to Table B1);

Completely dissolve the salt or base into a certain amount of distilled or deionised water;

Dilute with more distilled or deionised water to a final volume of desired range;

Thoroughly stir the solutions to obtain homogeneity.

**Table B1 - Chemical composition of 1 liter (1000 ml) solutions**

Salt /Base (purity: 99%)	Upstream solution (salt): 0.5M NaCl + 0.3M NaOH	Downstream solution (base): 0.3M NaOH
NaOH (g/liter)	12.121	12.121
NaCl (g/liter)	29.515	0



**BLANK PAGE**

## Appendix C – Accompanying Specimen for Pore Solution Extraction

**Accompanying Specimen:** The “accompanying specimen” is a disc like specimen that is cut off from the same cylinder or core as used for migration test. For laboratory cast and wet cured cylinders, the thickness of the specimen can be in between 25-30 mm. For cores made from structures, the thickness can be extended to but no more than 50 mm.

**Vacuum saturation:** The “accompanying specimen” is vacuum saturated with 0.3M NaOH solution together with the test specimens in the same vacuum container, following the procedure as described in 2.7. (Conditioning of Specimens).

**Pore solution extraction:** The chemical composition of the pore solution of the tested material will be used together with the migration measurements by the durability model for ionic diffusivity analyses. Pore solution extraction needs specially designed assembly. Figure C1 shows the assembly that has been used in the Concrete-Chemical Laboratory of Laval University. The crushed samples are placed into the hole on the steel cell, and a compressive loading is continuously applied onto the steel cylinder until enough pore solution is squeezed out and collected by the syringe. The minimum quantity of the pore solution needed for analyses is 2 ml. If necessary, more than one times of extraction can be made for the samples crushed from the same specimen in order to obtain sufficient quantity of the pore solution. The pore solution will be analyzed by using Atomic Absorption analyzer and Ion Chromatography as well as pH titrator to obtain the contents of the whole ionic family in the pore solution. The following cations and anions should be analyzed for ordinary Portland cement concrete samples: Na, K, Ca, SO<sub>4</sub>, Cl, OH. For concretes containing calcium nitrite-based corrosion inhibitors, the pore solution analyses should also include nitrite and nitrate ions (NO<sub>2</sub>, NO<sub>3</sub>).

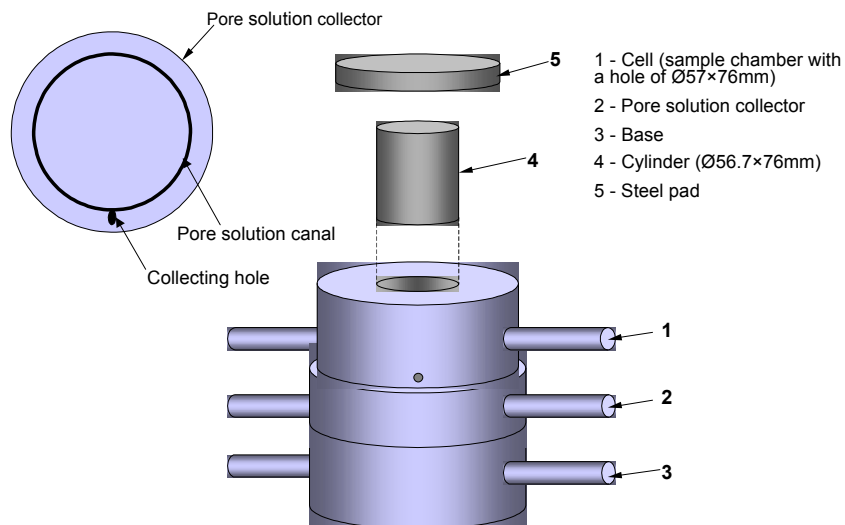


Figure C 1 - Assembly for pore solution extraction.

**BLANK PAGE**



## **Appendix D - Recent Advances in the Determination of Ionic Diffusion Coefficients Using Migration Test Results**

Published in RILEM Proceedings 58 – CONMOD 2008, Delft, The Netherlands, E. Schlangen and G. de Schutter, eds., p. 65-78, 2008.

**BLANK PAGE**

## Recent advances in the determination of ionic diffusion coefficients using migration test results

E. Samson <sup>(1)</sup>, J. Marchand <sup>(1,2)</sup>, Henocq P. <sup>(1)</sup>, and P. Beauséjour <sup>(2)</sup>

(1) SIMCO Technologies Inc., Québec, Canada

(2) Laval University, Civil Eng. Dept., Québec, Canada

### Abstract

Since the introduction of ASTM C1202, the so-called “rapid chloride permeability test”, accelerated methods based on the application of an external electrical potential have been commonly used to evaluate ionic diffusion properties of saturated hydrated cement systems. In some cases, these tests are integrated in a quality control program and results simply serve to assess the variability of a concrete from one production to another. In other cases, current data are analyzed to estimate the ionic diffusion coefficients of the material. Although the calculation method tends to vary from one laboratory to another, most approaches share a common feature. They all tend to be based on the assumption that ions move so quickly throughout the hydrated cement paste pore structure that chemical reactions can be neglected in the analysis. This hypothesis is quite convenient since it contributes to simplify considerably the analysis. In the present paper, a series of experimental test results clearly demonstrate the invalidity of this assumption, particularly in the cases of chloride ions. A new approach to analyze current data is then presented. This method allows taking into account the transport of all species and the influence of chemical reactions that may occur during the experiment. A series of numerical tests also emphasize the dominant role of the initial pore solution on the analysis.

### 1. Introduction

Ever since steel corrosion started to be a concern, numerous attempts have been made to develop models to predict the rate of contaminant ingress (such as chlorides) and thus assess the long-term durability of reinforced concrete structures. Most of the approaches so far proposed in the scientific literature are based on the assumption that the penetration of external chemicals in concrete is mainly driven by diffusion. In order to feed these models, experimental methods were also simultaneously developed to evaluate the diffusion coefficient, which drives the diffusion mechanism. The fact that the kinetics of ion diffusion in ordinary concrete mixtures is relatively slow prompted the development of accelerated methods, with the objective of determining the transport properties within a short timeframe.

This led to the apparition of accelerated tests where an external electrical potential is applied on a diffusion cell to accelerate the rate of penetration of chloride ions in the sample. Historically, the first accelerated test procedure was published by AASHTO under the designation T277. In 1991, ASTM adopted a slightly modified version of the procedure.

ASTM 1202, also known as the rapid chloride permeability test, rapidly gained in popularity. Since then, numerous other variations of the test were developed. While most of these methods do not provide for quantitative evaluation of the diffusion coefficient, they are still used to qualitatively estimate the ionic transport properties of saturated concrete.

The current trend in the construction industry is to specify materials based on a performance specification approach, where a given service life (e.g. 75 years) is targeted. This emphasizes the need for developing methods that would provide a reliable assessment of diffusion coefficients. Moreover, current standard methods are generally believed to be too favourable to materials incorporating cementitious admixtures while they give poor results for concrete prepared with calcium nitrite corrosion inhibitors [1]. The ASTM C1202 and AASHTO T277 methods were also found to poorly correlate with results obtained with the AASHTO T259 90-day salt ponding test [2], which questions their ability to be used in any performance-based specification protocol.

While the experimental aspects of the migration test are generally well defined, many different approaches have been developed to analyze the results and estimate the diffusion coefficients. Some steady-state methods are based on the flux of chlorides flowing across the material under the influence of the applied electrical potential [3] or on the variation of chloride concentration in the cathodic (upstream) solution reservoir [4]. Other methods are based on non-steady-state analyses. This is the case in reference [5], where a colorimetric method, using  $\text{AgNO}_3$  sprayed on a chloride bearing surface, is used to detect the depth of chloride penetration. But as shown on Figure 1 [data from reference 6], there is no correlation between the different methods. Similar results were also published in reference [7].

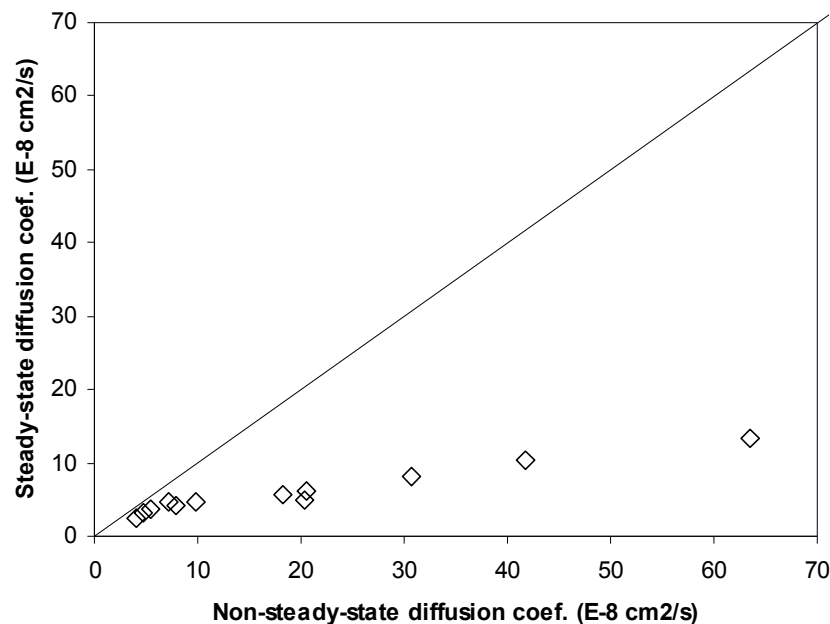


Figure 1: Correlation between steady-state and non-steady state

diffusion coefficients from accelerated tests [6]

A few years ago, the authors proposed a new multi-ionic approach to calculate diffusion coefficients from non-steady state migration test results [8]. This new method consisted in an analysis of electrical current measurements, which was based on the assumption that chemical reactions had a negligible influence on the transport of ions during a migration experiment. Such an hypothesis was justified by a dimensional analysis of the migration test that had indicated that the kinetics of ionic transport were much faster than that of chemical reactions. The method proved successful in estimating diffusion coefficients for chloride ingress [9] and sulfate exposure [10] cases.

Recent migration tests performed on samples of concrete mixtures made with cement bearing high levels of  $\text{Al}_2\text{O}_3$  and  $\text{SO}_3$  yielded diffusion coefficients that overestimated the ingress rate of chloride observed during ponding tests. These results suggested that chemical reactions could in certain cases have a significant effect on the mechanisms of ionic transport during a migration experiment. Such an observation was later confirmed by an investigation conducted by Voinitchi et al. [12]. In this study, the authors determined the distribution of chlorides across mortar samples that had been subjected to a migration experiment. The measured chloride levels were clearly above the level that could be expected if chlorides were solely dissolved in the liquid phase, a sign that chemical reactions occurred even in the presence of an applied electrical potential.

From these observations, a new model to analyze the migration test was developed. The method is still based on an analysis of the evolution of the current measured during the test, but it accounts for the potential influence of chemical reactions between the pore solution and the paste. The mathematical model is described in the next section. It is followed by a section dedicated to a sensitivity analysis. Its objective is to evaluate the influence of the main input parameters on the current calculated by the model. Finally, results from an actual migration experiment are compared to predictions made by the model.

## 2. Model description

The proposed model follows a multiionic approach based on a sequential split operator algorithm that separates ionic movement and chemical reactions. Details on the model can be found in papers [9, 10]. The ionic transport is described by the extended Nernst-Planck equation applied to saturated materials maintained under isothermal conditions<sup>8</sup>. This equation accounts for the electrical coupling as well as the chemical activity between ionic fluxes:

$$\frac{\partial c_i}{\partial t} - \text{div} \left( D_i \text{grad}(c_i) + \frac{D_i z_i F}{RT} c_i \text{grad}(\psi) + D_i c_i \text{grad}(\ln \gamma_i) \right) = 0 \quad (1)$$

where  $c_i$  is the concentration [mmol/L],  $D_i$  is the diffusion coefficient [ $\text{m}^2/\text{s}$ ],  $z_i$  is the valence number of the ionic species  $i$ ,  $F$  is the Faraday constant [96488.46 C/mol],  $\psi$  is the

<sup>8</sup> Typically, water content and temperature do not vary during a migration test.

electrodiffusion potential [V],  $R$  is the ideal gas constant [8.3143 J/mol/°K],  $T$  is the temperature [°K], and  $\gamma_i$  is the activity coefficient [-]. The activity coefficients in the model are evaluated on the basis of the Harvie, Moller and Weare (HMW) implementation of Pitzer's ion interaction model [12].

Seven ionic species are considered in the analysis of the migration test:  $\text{OH}^-$ ,  $\text{Na}^+$ ,  $\text{K}^+$ ,  $\text{SO}_4^{2-}$ ,  $\text{Ca}^{2+}$ ,  $\text{Al}(\text{OH})_4^-$ , and  $\text{Cl}^-$ . The diffusion coefficient of each ionic species is expressed as:

$$D_i = \tau D_i^o \quad (2)$$

where  $\tau$  is the tortuosity of the saturated material and  $D_i^o$  is the diffusion coefficient of the species in freewater. The values for  $D_i^o$  are constant at a given temperature and can be found in the literature (see for instance reference [13]). The objective of the test is thus to evaluate the tortuosity of the material. Since a migration test typically last less than one month, the change in transport properties due to hydration can be neglected, which means that  $\tau$  can be considered constant. This assumption is further supported by the fact that the test sample is immersed in an alkaline solution during the entire duration of the experiment. These conditions contribute to preserve the pore structure of the material throughout the test.

The electrodiffusion term involving the potential  $\psi$  in equation (1), is mainly responsible for maintaining the electroneutrality of the pore solution during diffusion. Its role is to balance the distribution of all species in solution so that there is no net accumulation of charge at any location in the pore solution. When a potential is applied, the term becomes more important than diffusion and drives the ions in the material<sup>9</sup>. To solve the diffusion potential  $\psi$ , the ionic transport equation is coupled to Poisson's equation, which relates the electrodiffusion potential in the material to the ionic profile distributions:

$$\text{div} (\tau \text{grad } \psi) + \frac{F}{\varepsilon} \left( \sum_{i=1}^N z_i c_i \right) = 0 \quad (3)$$

where  $\varepsilon$  [C/V/m] is the medium permittivity and  $N$  is the number of ions in the pore solution.

This system of  $N+1$  nonlinear equations is solved in 1D using the Newton-Raphson method with all equations solved simultaneously. The spatial discretization of this coupled system of equations uses the finite element method based on Galerkin's approach. An Euler implicit scheme is used to discretize the time-dependent part of the model. The numerical details are given in reference [10].

After having solved the set of equations (1)-(3) for a given time step, a chemical equilibrium module verifies each node of the finite element mesh to see if the chemical equilibrium between the ionic concentrations and the solid phases of the hydrated cement

---

<sup>9</sup> However, contrary to what as been assumed by many authors, the diffusion term cannot be neglected in the analysis. This point is further discussed in reference [8].

paste (see Table 1) is locally maintained for the equilibrium. The stability of each phase is modeled under the local equilibrium assumption according to:

$$K_m = \prod_{i=1}^N c_i^{v_{mi}} \gamma_i^{v_{mi}} \quad \text{with} \quad m = 1, \dots, M \quad (4)$$

where  $M$  is the number of solid phases,  $N$  is the number of ions,  $K_m$  is the equilibrium (or solubility) constant of the solid  $m$ ,  $c_i$  is the concentration of the ionic species  $i$ ,  $\gamma_i$  is its chemical activity coefficient, and  $v_{mi}$  is the stoichiometric coefficient of the  $i^{\text{th}}$  ionic species in the  $m^{\text{th}}$  mineral. If the solution is not in equilibrium with the paste, solid phases are either dissolved or precipitated to restore equilibrium.

Table 1: Mineral phases

Phase	Equilibrium relationship	$-\log(K_m)$
Portlandite	$K = (\text{Ca})(\text{OH})^2$	5.2
C-S-H	$K = (\text{Ca})(\text{OH})^2$	6.2
Ettringite	$K = (\text{Ca})^6(\text{OH})^4(\text{SO}_4)^3(\text{Al}(\text{OH})_4)^2$	44.0
Monosulfate	$K = (\text{Ca})^4(\text{OH})^4(\text{SO}_4)(\text{Al}(\text{OH})_4)^2$	29.4
Friedel's salt	$K = (\text{Ca})^4(\text{OH})^4(\text{Cl})^2(\text{Al}(\text{OH})_4)^2$	29.1

(...): chemical activity

The penetration of chloride in concrete structures leads to the formation of a chloride-AFm solid compound called Friedel's salt [14],  $3\text{CaO} \cdot \text{Al}_2\text{O}_3 \cdot \text{CaCl}_2 \cdot 10\text{H}_2\text{O}$ . Two different formation mechanisms were explored in reference [9]: dissolution/precipitation and ionic exchange. It was concluded that for diffusion cases (i.e. no potential applied), the ionic exchange mechanism is dominant. However, the chloride profiles measured after migration test on mortars in reference [11] clearly exhibit a sharp front penetrating the material. Similar measurements were obtained for this work. The presence of sharp fronts in a porous material is associated with the dissolution/precipitation mechanism [15]. Consequently, the formation of Friedel's salt in the material during a migration test is modeled according to equation (4). The mineral phases considered during the calculations are listed in Table 1. More details on the equilibrium values can be found in reference [9].

Given that the ionic fluxes are more important than what is typically observed during simple ponding experiments or for structures exposed to natural exposure conditions, the local equilibrium assumption may not be readily verified. To assess its validity, a procedure similar to the one presented in reference [10] is performed. The characteristic times [s] for the migration ( $t_\psi$ ) and chemical reaction ( $t_r$ ) processes are calculated according to the following relationships:

$$\begin{aligned}
 t_{\psi} &= \frac{RTl_o}{FD_{Cl}} \frac{L}{\Delta\psi} \\
 t_r &= \frac{1}{kA_r}
 \end{aligned}
 \tag{5}$$

where  $l_o$  is a characteristic migration length, taken as the typical element size: 1 mm. The parameter  $L$  corresponds to the total length of the sample used for the migration test: 50 mm. The potential difference applied during the test corresponds to  $\Delta\psi = 20V$ . The diffusion coefficient for chloride,  $D_{Cl}$ , is estimated at  $5 \times 10^{-11} \text{ m}^2/\text{s}$ , based on results published in reference [9]. The parameter  $k$  in the expression for the characteristic time associated with chemical reactions is the rate constant for the formation of Friedel's salt. Based on values published in [16], it is estimated at  $1 \times 10^{-8} \text{ mol}/\text{m}^2/\text{s}$ . The parameter  $A_r$  [ $\text{m}^2/\text{mol}$ ] corresponds to the reactive area in the material. Assuming a specific surface of  $100 \text{ m}^2/\text{g}_{\text{dry paste}}$  and  $30 \text{ g}/\text{kg}$  of monosulfates that convert into Friedel's salt yields a value of  $3.3 \times 10^5 \text{ m}^2/\text{mol}$  for  $A_r$  (see reference [10] for details). Using these parameters, one obtains characteristic times of 1250 s for the migration process and 300 s for the chemical reactions. Since chemical reactions have a shorter characteristic time compared to migration means that the local equilibrium assumption is still valid even when a potential is applied.

Once the concentration profiles are obtained, the current  $I$  [A] across the material can be calculated according to:

$$I = SF \sum_i^N z_i j_i \tag{6}$$

where  $S$  is the surface of the sample [ $\text{m}^2$ ], and  $j_i$  are the fluxes [ $\text{mol}/\text{m}^2/\text{s}$ ], given by:

$$j_i = -\phi D_i \text{grad}(c_i) - \phi \frac{D_i z_i F}{RT} c_i \text{grad}(\psi) - \phi D_i c_i \text{grad}(\ln \gamma_i) \tag{7}$$

with  $\phi$  standing for the porosity [ $\text{m}^3/\text{m}^3$ ].

### 3. Sensitivity Analysis

Simulations were performed with the model presented in the previous section to estimate the sensitivity of the current to selected parameters. Some parameters were set to determined values, as shown in Table 2. All the simulations were made with a time step of 900 s and a 140-element mesh that was refined at the boundaries.



Table 2: Parameter values for the sensitivity analysis simulations

Parameters	Values
Test geometry	
Sample thickness	50 mm
Sample diameter	100 mm
Boundary conditions	
NaOH ( $x=0$ )	300 mmol/L
NaOH ( $x=L$ )	300 mmol/L
NaCl ( $x=0$ )	500 mmol/L
NaCl ( $x=L$ )	0 mmol/L
Other ionic species ( $x=0$ and $x=L$ )	0 mmol/L
$\psi$ ( $x=0$ )	0 Volt
$\psi$ ( $x=L$ )	15 Volt
Material properties	
Porosity	13%
Initial portlandite content	30 g/kg
Initial C-S-H content	75 g/kg
Initial monosulfate content	35 g/kg

The objective of the first simulations was to estimate the effect of the chemical reactions on the current output. The simulations were performed with a tortuosity  $\tau=0.023$  (see eq. 2) which correspond to  $D_{OH}=12E-11$  m<sup>2</sup>/s. The following initial pore solution composition is considered: OH<sup>-</sup>:200.0, Na<sup>+</sup>: 100.0, K<sup>+</sup>: 100.1, SO<sub>4</sub><sup>2-</sup>: 2.0, Ca<sup>2+</sup>: 2.0 and Al(OH)<sub>4</sub><sup>-</sup>: 0.1 mmol/L.

Results are presented on Figure 2. They clearly show an important difference in the simulated currents when the chemical reactions are taken into account. Results indicate that estimating the tortuosity of a material on the basis of migration test data can induce a significant error when the reactions are neglected. In the present case, the current without the chemical reactions remained, until 300 hours, lower than the current with reactions. Neglecting the chemical reactions therefore translates in an overestimation of the diffusion coefficients in that case.

The next simulations were performed using the same initial pore solution composition. This time, different tortuosity values were tested: 0.023 ( $D_{OH}=12E-11$  m<sup>2</sup>/s), 0.028 ( $D_{OH}=15E-11$  m<sup>2</sup>/s) and 0.034 ( $D_{OH}=18E-11$  m<sup>2</sup>/s). Results are shown on Figure 3. Variations in the tortuosity have a proportional effect on the current, without much modification to the shape of the current curves. However, an increase in current was noted around 380 hours for the high tortuosity case. An analysis of this simulation revealed that the increase in current corresponds to the moment when the Friedel's salt reached  $x=L$ . The

chemical reactions associated with the presence of chlorides stopped, meaning that ions in solution were moving without the chemistry constraint, resulting in an increase in current.

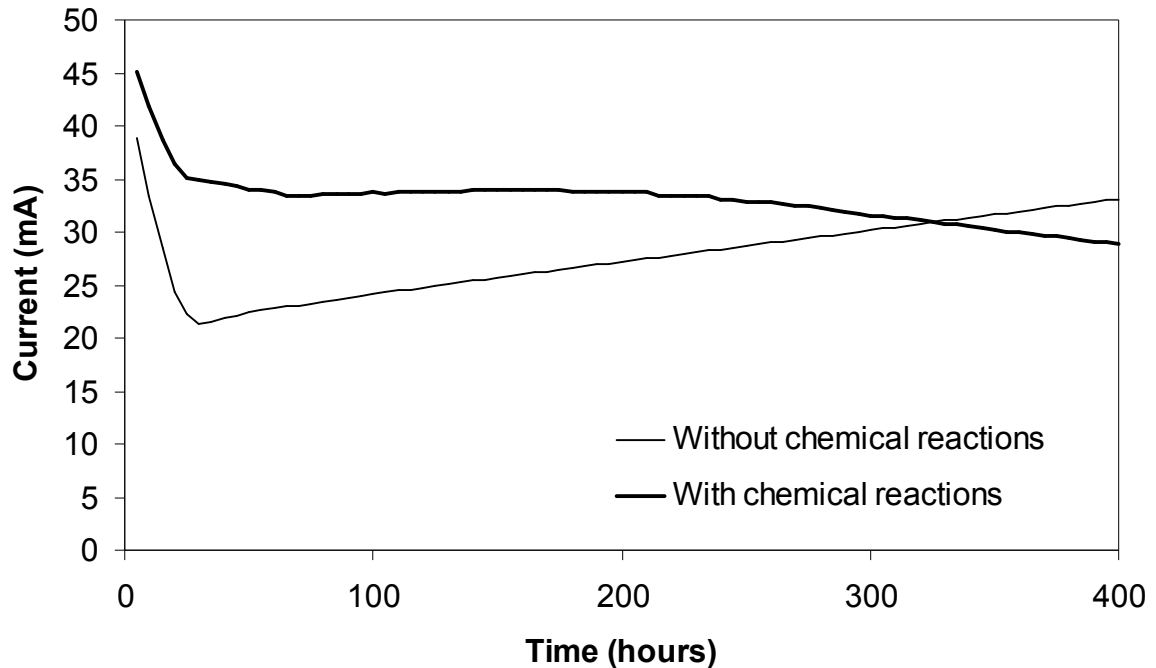


Figure 2: Simulated current with and without considering the chemical reactions

The third series of simulations consisted in testing the sensitivity to the initial pore solution composition. The pore solution used in the previous calculations corresponded to the base case. As shown in Table 3, two other pore solutions were tested, one with a higher ionic strength and one with a lower ionic strength. Simulation results are shown on Figure 4. From the simulated currents, it is clear that the initial pore solution has a strong influence on the initial output of the model. However, after 200 hours, all three current curves converge to the same value, corresponding to the case  $D_{OH}=15E-11$  m<sup>2</sup>/s on Figure 3. This indicates that at some point during the test, the parameter that determines the current value is the tortuosity. Other simulations showed that for poor quality materials (high tortuosity), the current reaches this stage earlier. For high quality concretes (low tortuosity), the influence of the initial pore solution is felt much longer on the current output and can easily reach 300 hours. Knowing that extracting the pore solution can be difficult in some cases, such as for low w/c concretes, these results indicate that ultimately, the test can be designed to minimize the impact of the pore solution composition. Even if this parameter carries a lot of experimental uncertainty, it will not affect the analysis if the test lasts long enough.

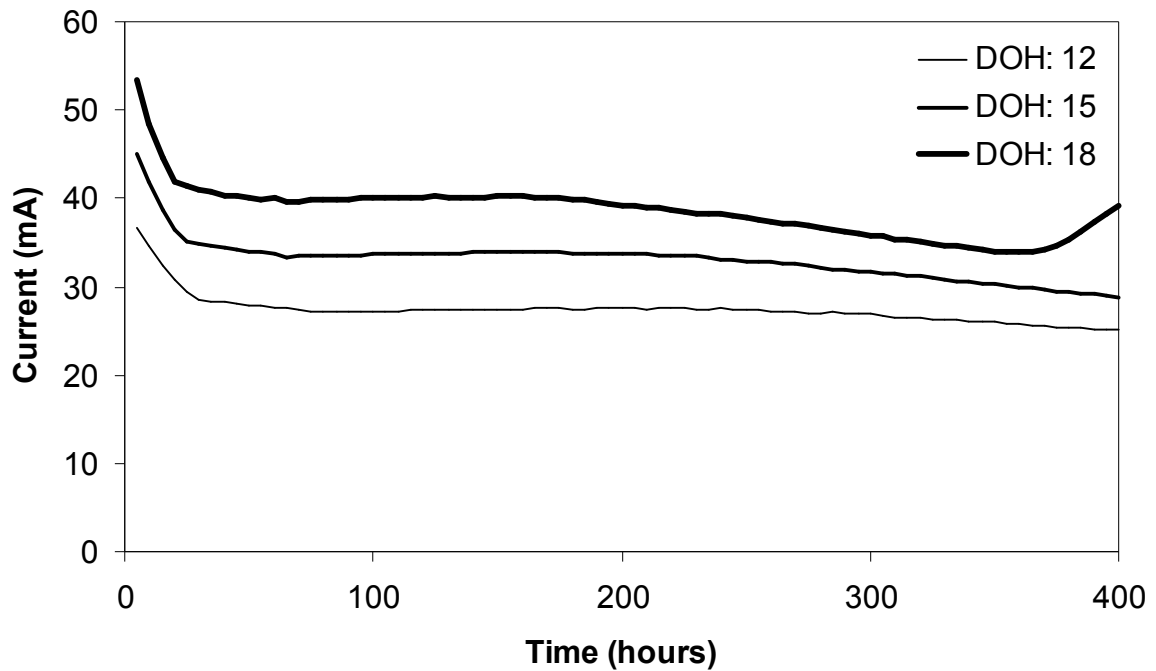


Figure 3: Effect of different diffusion coefficients on the simulated current

Table 3: Pore solutions for the sensitivity analysis

Ionic species	Pore solution composition (mmol/L)		
	Base Case	High	Low
OH <sup>-</sup>	200.0	300.0	100.0
Na <sup>+</sup>	100.0	200.0	0.0
K <sup>+</sup>	100.1	100.1	100.1
SO <sub>4</sub> <sup>2-</sup>	2.0	2.0	2.0
Ca <sup>2+</sup>	2.0	2.0	2.0
Al(OH) <sub>4</sub> <sup>-</sup>	0.1	0.1	0.1

Another set of parameters that may prove difficult to evaluate is the initial solid phase content of the paste (portlandite, C-S-H, monosulfates). While experimental techniques exist to assess the existence of phases in the hydrated paste, quantification is more problematic. The estimation can be based on models such as in reference [17]. As discussed in reference [9], the chloride entering the material reacts with the AFm to form Friedel's salt. Simulations were made with different AFm contents to quantify the impact of this parameter on the current output. The base case corresponded to the data presented in Table 2, where the initial AFm content was 35 g/kg of concrete. Other simulations were made with 30 and 40 g/kg of AFm. The results are shown on Figure 5 and indicate a very weak dependency on this parameter. Similar to the pore solution case, the difficulty associated with the evaluation of this parameter is overridden by its low impact of the model output.

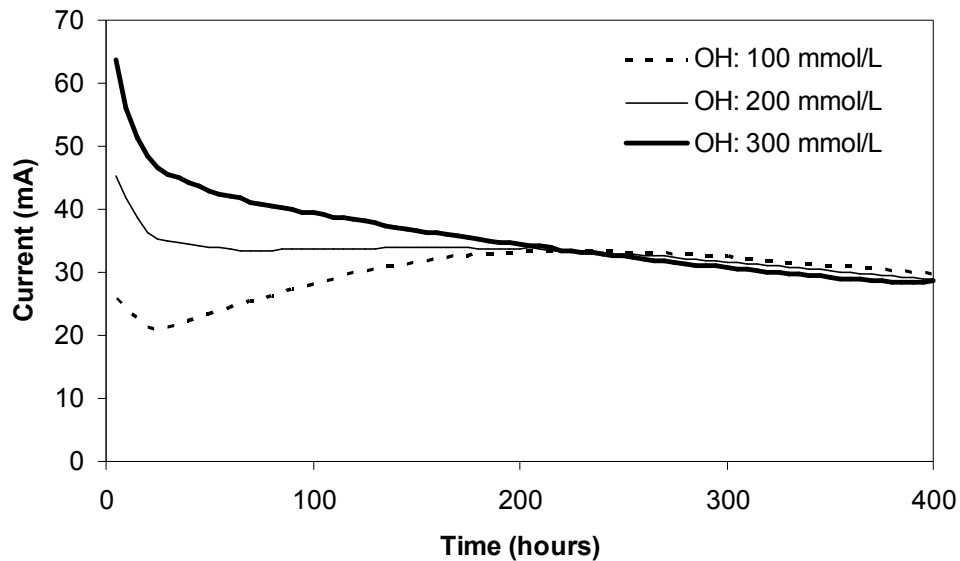


Figure 4: Effect of different pore solution compositions on the simulated current

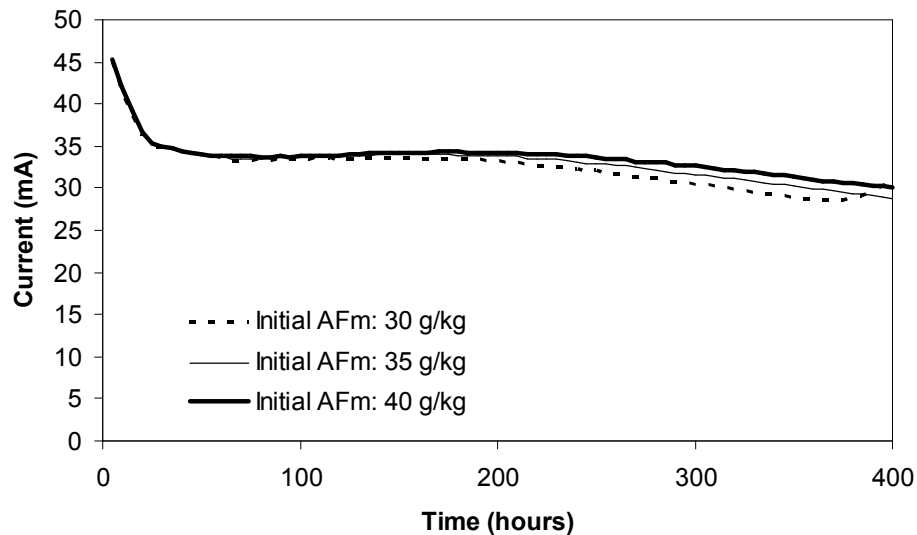


Figure 5: Effect of different initial AFm contents on the simulated current

#### 4. Experimental results

A migration test was performed on a concrete prepared at a 0.45 w/c ratio with ASTM Type I cement. Details on the mixture proportions and cement composition are given in Table 4. The material was cast in plastic cylinders (diameter: 10 cm, height: 20 cm) and demolded 24 hours later. After that, the cylinders were placed in a fog room (100% RH) for curing. The cylinders were cured for 28 days prior to testing.

After the curing period, two 50-mm discs were cut from one cylinder and saturated under vacuum in a 0.3 M NaOH solution for 24 hours to make sure that the samples are initially saturated. After saturation, the lateral surface of the discs was coated with a silicon gel. The discs were then mounted on the migration cells as shown on Figure 6. The cell/disc interface was also coated with silicon to ensure a watertight joint. Both compartments of the cells were filled with approximately 3 L of solution. The test solution on the upstream side of the cell was made of 300 mmol/L of sodium hydroxide (NaOH) and 500 mmol/L of sodium chloride (NaCl). The downstream cell was filled with a 300 mmol/L sodium hydroxide solution. During the test, an external 20 V potential was applied to the cell, which resulted in a 17.8 V potential across the samples due to the small resistance of the test solutions. The current passing through the samples was regularly measured over a 500-hour period.

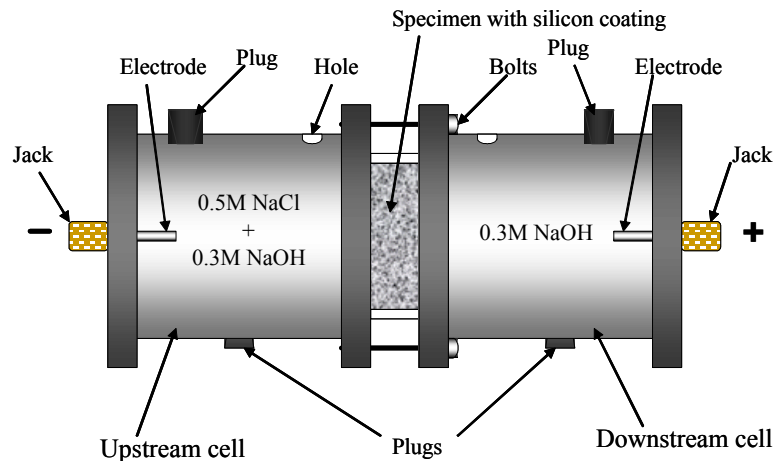


Figure 6: Migration test setup

Companion discs were cut from cylinders to perform additional tests after 28 days of curing in the fog room. The volume of permeable pores of the material (i.e. its porosity) was evaluated according to the ASTM C642 procedure. The result, presented in Table 4, is the average of two separate measurements.

The initial composition of the pore solution was obtained by extracting the solution under an applied external pressure [18]. The solution was collected in a syringe to limit contact with air. It was stored in a refrigerator until the analysis was performed. Before the analysis, the solution was diluted approximately 10 times to get sufficient solution for all the measurements. The concentrations in  $\text{OH}^-$  and  $\text{Cl}^-$  were evaluated by potentiometric titration and the cation concentrations ( $\text{Ca}^{2+}$ ,  $\text{Na}^+$ ,  $\text{K}^+$ ) were analyzed using ICP. The initial content concentration in  $\text{Al}(\text{OH})_4^-$  was estimated at 0.1 mmol/L since it was too weak to be measured after the solution dilution. Also, due to experimental errors, the extracted solution was not strictly neutral. The solution was balanced to respect the electroneutrality requirement. The results are presented in Table 4.

Table 4: Parameters used for the migration test

Parameter	Value	Parameter	Value
w/c	0.45	Porosity	12.3%
Cement Type	ASTM I	Initial pore solution	(mmol/L)
Mixture proportions	(kg/m <sup>3</sup> )	OH <sup>-</sup>	210.3
Cement	375	Na <sup>+</sup>	120.8
Water	169	K <sup>+</sup>	139.3
Fine aggregates	815	SO <sub>4</sub> <sup>2-</sup>	12.9
Coarse aggregates	925	Ca <sup>2+</sup>	1.6
Cement composition	(% mass)	Al(OH) <sub>4</sub> <sup>-</sup>	0.1
CaO	64.0	Cl <sup>-</sup>	27.1
SiO <sub>2</sub>	21.0	Initial solid phases	(g/kg)
Al <sub>2</sub> O <sub>3</sub>	5.9	Portlandite	23.5
SO <sub>3</sub>	3.3	C-S-H	68.0
Fe <sub>2</sub> O <sub>3</sub>	2.2	Monosulfates	28.5
K <sub>2</sub> O	0.41	Estimated tortuosity	0.0247
Na <sub>2</sub> O	0.22		

The initial solid phase content in the hydrated paste was estimated following a method similar to the one described in [10]. A cement hydration level of 65% after 28 days was assumed for the calculations of portlandite, C-S-H and monosulfates. The results are given in Table 4.

Using these parameters, the tortuosity factor was adjusted until a proper fit with the measured current values was reached. Results of the numerical simulations are presented in Figure 7. The simulated current was obtained with a tortuosity value of 0.0247, which gives the following diffusion coefficients for the different ionic species:  $D_{OH}=13.0E-11$  m<sup>2</sup>/s,  $D_{Na}=3.3E-11$ ,  $D_K=4.8E-11$ ,  $D_{SO_4}=2.6E-11$ ,  $D_{Ca}=2.0E-11$ ,  $D_{Al(OH)_4}=1.3E-11$  and  $D_{Cl}=5.0E-11$ . As seen on the figure, the model allows reproducing the main features of the measured current. Initially, a drop in the current is measured, until approximately 200 hours. The current is then stable for about 100 hours until it starts increasing after 300 hours. The model also predicts an initial drop in current but does not exhibit a stable value between 200 and 300 hours. After 350 hours, the model predicts an increase in current that matches the intensity of the measurements.

A simulation was also performed without considering the chemical reactions. The calculations were made with a tortuosity of 0.0247. As shown in Figure 7, the predicted current is in this case very different from the measured values. Apart from an initial drop, the current increases almost linearly after 25 hours.

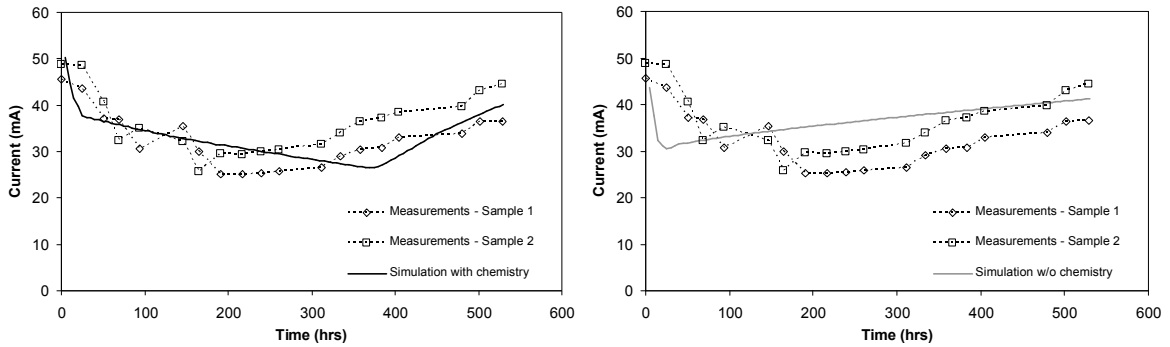


Figure 7: Comparison of the numerical current with the measurements

To validate the tortuosity value estimated with the migration test, companion samples were exposed to a sodium chloride solution for 90 days. One cylinder was taken from the fog room after 28 days of curing and cut in the middle. The two pieces were sealed with wax, except for the cut surfaces, in order to enforce 1D chloride ingress during the test. The samples were then immersed in a 0.5M sodium chloride solution. Large volume containers (30 – 40 L) were used to maintain constant exposure conditions. Furthermore, the pH of the immersion solution was measured on a regular basis. When its value reached 10.5, the solution was renewed, thus maintaining constant boundary conditions throughout the experiment. After the exposure period of 90 days, the chloride profiles were measured following a modified version of the ASTM C1152 layer-by-layer acid dissolution procedure using 3 mm depth increments.

Simulations were then made to reproduce the measured profiles using the parameters in Table 4. As mentioned in section 2, the chloride binding is modeled according to the ionic exchange mechanism described in reference [9] since no external potential was applied in this case. The results given in Figure 8 show a very good match between the measurements and the simulated chloride profile.

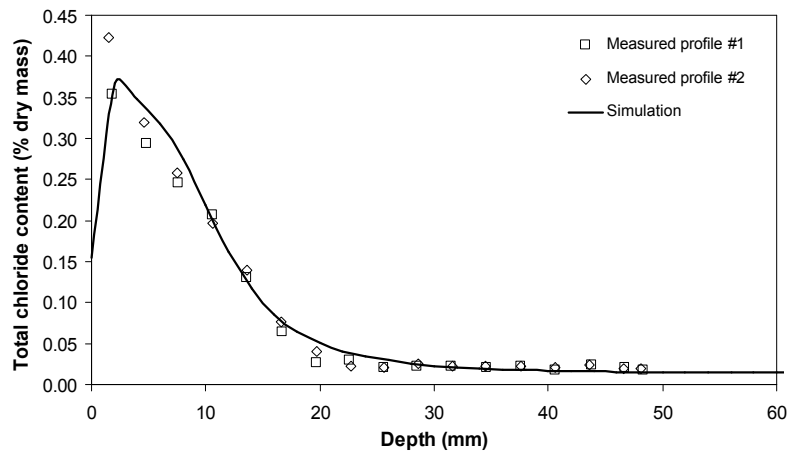


Figure 8: Chloride profiles after a 90-day exposure to 0.5M sodium chloride

## 5. Conclusion

The paper presented a new approach to model the migration test. The model is based on a multiionic approach that considers the coupling between ionic species according to the Nernst-Planck equation. Following results found in the literature, the model also considers the chemical reaction between chloride and the paste occurring during the test. The formation of Friedel's salt is modelled with a dissolution/precipitation mechanism. The test is analyzed by comparing the simulated currents with the ones measured during a migration experiment.

A sensitivity analysis emphasized the major influence of the chemical reactions during a migration test. The numerical results showed that neglecting the chemical reactions could lead to an overestimation of the tortuosity of the material. Other numerical simulations showed that the initial pore solution influences the current at the beginning of the analysis but this influence gradually disappears as the experiment goes on. These results indicate that if the composition of the pore solution is not known precisely, the experimental uncertainty can be minimized if the migration tests last long enough.

Finally, the model was compared to migration test results performed on a 0.45 Type I concrete. The model was able to reproduce the initial drop in current measured during the test as well as the increase in current at the end. The value of tortuosity that reproduced the measured current was then used to simulate an immersion test where concrete samples were exposed for 90 days to a 0.5M sodium chloride solution. The simulation results matched well with the measured chloride profiles.

## 6. References

1. Bassuoni M.T., Nehdi M.L., Greenough T.R., 'Enhancing the reliability of evaluating chloride ingress in concrete using the ASTM C1202 rapid chloride permeability test', *Journal of ASTM Int.* 3(3) (2006).
2. McGrath P.F., Hooton R.D., 'Re-evaluation of the AASHTO T259 90-day salt ponding test', *Cement and Concrete Research* 29 (1999) 1239-1248.
3. Friedmann H., Amiri O., Aït-Mokhtar A., Dumargue P., 'A direct method for determining chloride diffusion coefficient by using migration test', *Cement and Concrete Research* 34 (2004) 1967-1973.
4. Truc O., Ollivier J.P., Carcassès M., 'A new way for determining the chloride diffusion coefficient in concrete from steady-state migration test', *Cement and Concrete Research* 30 (2000) 217-226.
5. Baroghel-Bouny V., Belin P., Maultzsch M., Henry D., 'AgNO<sub>3</sub> spray tests: advantages, weaknesses, and various applications to quantify chloride ingress into concrete. Part 2: Non-steady-state migration tests and chloride diffusion coefficients', *Materials and Structures* 40 (2007) 783-799.



6. Yang C.C., 'A comparison of transport properties for concrete using the ponding test and the accelerated chloride migration test', *Materials and Structures* 38 (2005) 313-320.
7. Tong L., Gjrv O.E., 'Chloride diffusivity based on migration testing', *Cement and Concrete Research* 31 (2001) 973-982.
8. Samson E., Marchand J., Snyder K., 'Calculation of ionic diffusion coefficients on the basis of migration test results', *Materials and Structures* 36 (2003) 156-165.
9. Samson E., Marchand J., 'Multiionic approaches to model chloride binding in cementitious materials', in Proceedings of the 2<sup>nd</sup> Int. Symp. On Adv. In Concrete Through Science and Engineering (Qubec, Canada), Marchand et al. Eds, RILEM Proceedings 51 (2006) 101-122.
10. Samson E., Marchand J., 'Modeling the transport of ions in unsaturated cement-based materials', *Computers and Structures* 85 (2007) 1740-1756.
11. Voinitchi D., Julien S., Lorente S., 'The relation between electrokinetics and chloride transport through cement-based materials', *Cement and Concrete Composites* 30 (2008) 157-166.
12. Zhang G., Zheng Z., Wan J., 'Modeling reactive geochemical transport of concentrated aqueous solutions', *Water Resources Research* 41 (2005) doi: 10.1029/2004WR003097.
13. Li Y.H., 'Diffusion of ions in sea water and in deep-sea sediments', *Geochimica et Cosmochimica Acta* 38 (1974) 703-714.
14. Brown P., Bothe J., 'The system CaO-Al<sub>2</sub>O<sub>3</sub>-CaCl<sub>2</sub>-H<sub>2</sub>O at 23±2 °C and the mechanisms of chloride binding in concrete', *Cement and Concrete Research* 34 (2004) 1549-1553.
15. Rubin, J., 'Transport of reacting solutes in porous media: relation between mathematical nature of problem formulation and chemical nature of reactions', *Water Resources Research* 19(5) (1983) 1231-1252.
16. Lichtner P.C., Pabalan R.T., Steefel C.I., 'Model calculations of porosity reduction resulting from cement-tuff diffusive interaction', *Mat. Res. Soc. Sympos.* 56 (1998) 709-718.
17. Papadakis V.G., 'Experimental investigation and theoretical modeling of silica fume activity in concrete', *Cement and Concrete Research* 29 (1999) 79-86.
18. Barneyback R.S., Diamond S., 'Expression and analysis of pore fluid from hardened cement paste and mortars' *Cement and Concrete Research* 11 (1981) 279-285.

**BLANK PAGE**

**Appendix E - Determination of the Water Diffusivity of Concrete  
Using Drying/Absorption Test Results**

Published in the Journal of the ASTM International, Vol. 5, No. 7, 2008

**BLANK PAGE**

## **Determination of the water diffusivity of concrete using drying/absorption test results**

Eric Samson<sup>1</sup>, Keyvan Maleki<sup>1</sup>, Jacques Marchand<sup>1,2</sup>, Tiewei Zhang<sup>1</sup>

(1) SIMCO Technologies Inc., 1400 boul. du Parc-Technologique, Suite 203  
Quebec City, (QC), Canada, G1P 4R7

(2) Department of Civil Engineering, Laval University  
Quebec City, (QC), Canada, G1K 7P4

### **Abstract**

Experimental procedures such as ASTM C1585 and ISO12572 have been recently developed to determine the rate of moisture transmission through hydrated cement systems. However, these methods do not provide an actual transport parameter that can be used in chloride ingress models to predict the service-life of concrete structures. This study focused on the development a reliable method to measure the nonlinear moisture diffusivity of concrete. The approach is based on the analysis of drying and wetting experiments performed with concrete samples of different thicknesses. The transport parameter is obtained by using Richards' water transport model to analyze the mass variations measured during the tests. The method was tested over a wide range of different concrete mixtures produced with different water/cement ratios. Results indicate that the nonlinear function used to reproduce the mass variation curves must exhibit a strong increase for high water content values. The water diffusivity equation derived from this analysis allows reproducing the behavior of concrete during both the drying and absorption experiments using the same water transport model.

**Key words:** water diffusivity, drying test, Richards' model, absorption, durability, concrete.

## **1. Introduction**

In recent years, the increasing number of concrete structures showing signs of degradation triggered the development of advanced modeling techniques to predict service-life in harsh environments. In the case of chloride ingress, the simplified Fick's second law fitting is still widely used [Ghods05]. But new models were recently developed to take into account several aspects of ionic transport that are overlooked using Fick's approach. As shown in references [Saetta93, Nagesh98, Hansen99, Swaddiwudhipong00, Martin01], models are now coupled with energy and moisture conservation equations to estimate water content and temperature fields and their effect on ionic transport. More recently, multiionic models added

electrostatic ionic coupling and complex chemical interactions [Masi97, Samson07] to refine the description of ionic transport.

Increasing the complexity of models leads to an increase in the number of parameters needed to perform durability predictions. In that regard, the ionic diffusion coefficient has received most of the attention. Tests to evaluate this parameter are usually based on a modified version of the Rapid Chloride Permeability Test (ASTM C1202), which consists in applying a voltage across a sample to accelerate ionic movement. The diffusion coefficient can be estimated on the basis of steady state measurements of chloride concentration across the setup [McGrath96, Tong01] or electrical current measured during the experiment [Samson03, Friedmann04].

Despite their practical importance, the properties that characterize water transport of concrete have received little attention. Similar to the ASTM C1202 procedure, there are test methods that allow qualitative comparisons between materials, such as ISO12572 and ASTM C1585. In the ISO12572 case, cylindrical samples are exposed to humidity gradients. One face is maintained close to water, thus creating a high humidity boundary condition. The other face is exposed to a lower humidity environment. The humidity gradient drives water through the sample. The mass of the set-up is measured until it is stable. It provides an evaluation of the steady-state moisture flux across the sample.

The ASTM C1585 procedure consists in exposing a pre-dried cylindrical sample to water, which causes the cementitious material to absorb the liquid. The samples are conditioned to 50% - 70% relative humidity. During absorption, mass is recorded on a regular basis. The experimental data, expressed in  $\text{mm}^3/\text{mm}^2$ , are then plotted against the square root of time. The curve thus obtained usually shows two linear segments, respectively called initial and secondary absorption. The slope of the initial absorption is called the sorptivity and can be used to compare the absorption of different cementitious materials.

However, these test methods do not provide a parameter that, similarly to the diffusion coefficient, can be used to predict the spatial distribution of water content or humidity at different times as a function of the material characteristics and exposure conditions. In order to make service-life and durability predictions, it is necessary to evaluate a water diffusivity  $D_w$  that is then used as an input parameter in an ionic transport model to take into account the effect of water flow on ionic transport.

Few methods have been designed to directly evaluate water diffusivity. Most attempts were made by investigating the ingress of absorbed water in oven-dried construction materials using the NMR technique (see Figure 1) [Pel96]. Carmeliet et al. [Carmeliet04] obtained similar results with X-ray projection. In both cases, the profiles were analyzed using a Boltzmann transformation to yield the liquid water diffusivity. The main drawback of these methods is the use of expensive experimental apparatus that can only be afforded by universities and large research laboratories.

This paper presents a new method to evaluate the water diffusivity of cementitious materials. The proposed approach gives a parameter that can directly be implemented in an ionic transport model to simulate the evolution of water profiles in concrete structures and their service-life.

## 2. Water transport modeling

Before presenting the test method, the water transport model used for the analysis is presented since it affects the way the test method will be devised.

Two main approaches have been used to model moisture movement in hydrated cement systems. The first one is based on a thorough description of all the phases involved in the process: liquid (aqueous solution), water vapor and dry air. Multiple mass conservation equations are involved to obtain the description of the three fields. The second approach can be derived from the first one under simplifying assumptions. It usually leads to a single equation (called the Richards' equation), which allows the water content field to be evaluated.

Mainguy et al. [Mainguy01] relied on the multiphase approach to describe moisture movement under isothermal conditions. The mass balance equations for the three phases (liquid water ( $l$ ), dry air ( $a$ ) and water vapor ( $v$ )) that can be present in partially saturated concrete are given as:

$$\frac{\partial(\phi\rho_l S_l)}{\partial t} + \text{div}(\phi S_l \rho_l v_l) + \mu_{l \rightarrow v} = 0 \quad (\text{liquid}) \quad (8)$$

$$\frac{\partial(\phi\rho_v(1 - S_l))}{\partial t} + \text{div}(\phi(1 - S_l)\rho_v v_v) - \mu_{l \rightarrow v} = 0 \quad (\text{water vapor}) \quad (9)$$

$$\frac{\partial(\phi\rho_a(1 - S_l))}{\partial t} + \text{div}(\phi(1 - S_l)\rho_a v_a) = 0 \quad (\text{dry air}) \quad (10)$$

where  $\phi$  is the porosity,  $\rho_i$  is the density of phase  $i$ ,  $S_l$  is the liquid water saturation,  $v_i$  is the velocity of constituent  $i$ , and  $\mu_{l \rightarrow v}$  is the rate of liquid water vaporization. The liquid phase velocity is given by the Darcy state law:

$$\phi v_i = -\frac{K}{\eta_i} k_{ri}(S_l) \text{grad}(p_i) \quad (11)$$

where  $K$  is the intrinsic permeability of the porous material,  $\eta_i$  is the dynamic viscosity of phase  $i$ ,  $k_{ri}(S_l)$  is the relative permeability and  $p_i$  is the pressure. The dry air and vapor phases state law is given by Fick's relationship, expressed as:

$$\phi_g \rho_j v_j = \phi_g \rho_j v_g - \rho_j \frac{D}{C_j} f(S_l, \phi) \text{grad}(C_j) \quad (12)$$

where  $v_g$  is the gas molar-averaged velocity satisfying Darcy's law,  $D$  is the diffusion coefficient of water vapor or dry air in wet air,  $f$  is the resistance factor accounting for both the tortuosity effect and the reduction space offered to the diffusion of gaseous constituents, and  $C_j$  is the ratio  $p_j/p_g$  with  $j = a$  or  $v$  [Degiovanni87]. A similar model was developed by Selih [Selih96]. The model developed by Mainguy et al. [Mainguy01] has been found to properly reproduce isothermal drying test results. However, this approach is marginally useful in durability analyses, mainly because of the rather large number of parameters that need to be determined.

The simplified approach is often selected to describe the variation in water content within cement-based materials. One of the main differences between two approaches is the assumption that gas pressure is uniform over the material and is equal to atmospheric pressure. Under this hypothesis, it has been shown [Whitaker98, Samson05] that the water content can be evaluated on the basis of Richards' equation:

$$\frac{\partial w}{\partial t} - \text{div}(D_w \text{grad}(w)) = 0 \quad (13)$$

where  $w$  is the volumetric water content and  $D_w$  is the nonlinear water diffusivity parameter. Using this approach, the average velocity (flux) of the fluid phase is given by:

$$\mathbf{v} = -D_w \text{grad}(w) \quad (14)$$

Expressions for  $D_w$  based on a mechanistic description of fluid flow in unsaturated materials yield relationships involving multiple parameters such as the permeability, which are known to be difficult to evaluate in cementitious materials [Whitaker98, Samson05]. Authors have instead proposed to use simplified nonlinear relationship such as [Hall94]:

$$D_w = A \exp(Bw) \quad (15)$$

where  $A$  and  $B$  must be determined experimentally and  $B$  is positive.

Instead of using water content as state variable, other authors have chosen to model the relative humidity field  $h$ , under the assumption that the driving force can be expressed as:  $\mathbf{v} = -D_h \text{grad}(h)$ . In that case, equation (13) can be written as [Bazant71, Xi94]:

$$\frac{\partial w}{\partial h} \frac{\partial h}{\partial t} - \text{div}(D_h \text{grad}(h)) = 0 \quad (16)$$



Again, the moisture diffusivity parameter is a nonlinear function that can be expressed as [Xi94]:

$$D_h = \alpha + \beta(1 - 2^{-10^\gamma(h-1)}) \quad (17)$$

where  $\alpha$ ,  $\beta$  and  $\gamma$  are parameters that must be determined experimentally.

The analysis methods presented in references [Pel96, Carmeliet04] are based on Richards' equation (13) using an exponential expression for  $D_w$  (equation (15)). Also, the water content variable is directly part of the ionic mass conservation equations for unsaturated materials (see for instance references [Samson07, Samson05, Bear91]). Consequently, Richards' equation (13), coupled with the exponential water diffusivity (15), were selected to support the analysis method that was developed. The objective is to devise an experimental method that will allow determining  $A$  and  $B$  (15). It will then be possible to evaluate the water content in a concrete structure and the fluid flow that affects chloride ingress.

### 3. Test method

The test method presented in this study was not the first one devised by the authors. A first attempt consisted in exposing concrete samples to two different relative humidities, 50% and 75%, in closed boxes containing the proper salt solutions. The samples were initially saturated and were thus drying upon contact with the lower humidity environment. The mass of the samples was measured on a regular basis. The two sets of experimental mass-loss curves (50% and 75%) were then fitted using Richards' equation (13) by adjusting  $A$  and  $B$ . However, the method proved imprecise because the mass loss curves for both humidities were in some cases very close to each other, making it difficult to find unique values for  $A$  and  $B$ . Also, the analysis proved very sensitive to the boundary conditions used for the calculations, and the method itself did not provide any indication to set the water content value at the material/environment interface.

A new test method had to be developed to circumvent these problems. The new method is still based on drying initially saturated samples. It consists in exposing two sets of concrete disks to a 50% RH environment. The first set consisted in 5-cm thick samples while the other was made of 1-cm thick samples. Three samples per set were used. The samples were cut from cylinders that had been cured in a fog room for more than a year. IT was assumed that the samples were saturated before the test started. After being cut, the samples were measured (diameter and thickness) and weighed in air and in water to evaluate their volume. The samples were then coated with silicon on their round surface. Both flat surfaces were kept wet with cloths while the coating was drying. The samples were then placed in a 50% RH room, where the drying process starts. Since only the round surface was coated, the disks were drying from both flat faces. This particular set-up enforces 1D moisture transport and is

symmetrical with regard to the middle of the disk. To ensure proper air flow around the samples, they were placed on thin supports, as shown on Figure 2, or placed on their side.

Once in the 50%-RH room, the samples are weighted on a regular basis according to the following schedule:

- Day 1 to 2: two times per day with at least 6 hours between measurements,
- Day 2 to 7: once per day,
- Day 8 to 30: three times per week with at least two days between measurements,
- After 30 days: two times per week with at least three days between measurements.

The test was stopped when the masses of the 1-cm samples were stable, i.e. when four consecutive measurements were equal or oscillate within 0.01 g.

The concrete tested in this study are shown in Table 1. Materials A to D were ordinary mixtures made with CSA Type 10 cement while material E was made with ASTM Type I cement incorporating 20% type F fly ash. In all cases, the materials were hydrated at least one year in a fog room prior to testing. The duration of the test depends on the quality of the material. The low quality concrete D reached equilibrium after approximately 40 days while the test lasted around 70 days for the concrete with fly ash.

Typical results obtained on a concrete made at a water/cement ratio of 0.4 with CSA Type 10 cement are shown on Figure 3, where the mass loss is plotted against time. Prior to the test, this particular concrete had been kept in a fog room for three years. The mixture characteristics are given in Table 1 and correspond to material A. The results show that while the mass stabilizes rather rapidly for the 1-cm samples, it keeps evolving for the 5-cm samples. For this particular material, it took about 60 days to reach equilibrium for the thin samples.

#### 4. Analysis

The analysis of the test results using Richards' equation (13) requires determining the initial water content of the material. Since the samples are initially saturated, it is assumed that the initial value of  $w$  corresponds to the porosity. It is evaluated on companion samples using the ASTM C642 standard procedure, which yields the volume of permeable voids. A porosity of  $13.06 \text{ m}^3/\text{m}^3$  was measured for concrete A.

The boundary conditions needed to solve equation (13) are provided by the equilibrium value reached with the 1-cm samples. The equilibrium water content is given as:

$$w_{eq} = \phi - \frac{\Delta M_{eq}}{V} \quad (18)$$

where  $\phi$  is the porosity [ $\text{cm}^3/\text{cm}^3$  or  $\text{m}^3/\text{m}^3$ ],  $\Delta M_{eq}$  is the equilibrium mass loss [grams] and  $V$  is the volume of the sample [ $\text{cm}^3$ ]. The calculations are made using the average equilibrium value and the average volume of the three 1-cm samples. This value corresponds to the data at 50% RH for a desorption isotherm. For the case illustrated on Figure 3, the water content at equilibrium is given by  $w_{eq} = 0.1306 - 4.6/89.3 = 0.079 \text{ m}^3/\text{m}^3$ . This value is applied as a Cauchy boundary condition on both sides of the samples:

$$v_n = h_w(w - w_{eq}) \quad (19)$$

where  $v_n$  is the normal flux imposed at  $x=0$  and  $x=L$ , and  $h_w$  is the exchange coefficient. Figure 4 illustrates the simulation boundary and initial conditions. Because of the symmetry around  $x=L/2$ , it is possible to simulate half the domain by imposing a null flux condition at the center of the material.

The validity of the equilibrium value has been checked using concrete samples prepared at the same water/cement ratio and using the same cement as for mixtures B, C, and D. The cylindrical samples had a 14 mm diameter and a 6 cm length. They were placed in closed boxes where the humidity was maintained at 53% using an  $\text{Mg}(\text{NO}_3)_2$  saturated salt solution. They were maintained in the boxes for 14 months and then weighed to evaluate the remaining water content. The results are given in Table 3. There is a good agreement between the values for materials B and D. The equilibrium value for material C obtained from the 14-month experience is actually lower than the water content of the more porous material D. The value must be at the lower end of the spectrum and is not considered representative. The discrepancy between the results of these tests with the drying experiment could also be explained by the small size of the cylindrical samples. Given the results obtained for materials B and D, the equilibrium values obtained at the end of the drying tests using the data from the 1-cm series can be considered stable.

Simulations are made to reproduce the average mass loss curve of both data sets in order to find the values of  $A$ ,  $B$  and  $h_w$ . Richards' equation is solved using the finite element method. A 3600 s time step is used for the time discretization. At every 5 time steps, the mass loss is calculated from the numerical water content profile according to:

$$\Delta M|_t = \left[ \int_0^L (\phi - w) dx \right] S \quad (20)$$

where  $\Delta M|_t$  is the mass loss evaluated at time  $t$  (grams),  $L$  is the average thickness of the samples (cm), and  $S$  is the averaged exposed surface ( $\text{cm}^2$ ). The optimization of the parameters is made by minimizing the difference between the experimental and numerical area under both mass loss curves.

The first simulations emphasized the effect of the exchange coefficient  $h_w$ . This parameter mainly influences the first hours of the drying simulations but does not have a large influence

on the overall optimization when all the duration of the test is considered. A good match with the first measurements is obtained with  $h_w=10\times 10^{-8}$  [m/s] for all concrete mixtures that were tested. Very few values for  $h_w$  could be found in the literature. The value of  $h_w=10\times 10^{-8}$  [m/s] is in line with the data found in reference [Sakata83]. However, the author [Sakata83] noted an influence of the w/c ratio on  $h_w$ , which was not observed in the present drying tests. It was also noted that in the first few hours of the drying tests, the model was in most cases underestimating the measured mass loss. This was attributed to an initial freewater drying due to the presence of water droplets on the material surface.

The analysis of the test results also showed that interestingly, the mixture composition of the concrete does not have a strong influence on the parameter  $B$ . In all cases, the best fit was obtained with  $B$  values ranging from 75 to 85 and had no particular correlation with the type of material. Accordingly, it was assumed that  $B=80$  for all concrete mixtures. Similar tests made on mortar samples gave a  $B$ -value around 50. The ratio 80/50 roughly corresponds to the volumetric paste content ratio between both materials, i.e. 30% for concretes and 50% for mortars. This suggests that  $B$  depends mainly on the paste content. This still needs to be verified with drying tests made on hydrated paste samples. The optimization is thus performed solely on parameter  $A$  in order to reproduce the 1-cm and 5-cm test series. The optimization procedure was automated to find the value of  $A$  that minimizes the area under the numerical and experimental mass loss curves for the 1-cm and 5-cm test series. The simulation results for the experimental data shown in Figure 3 are given in Figure 5. Both series exhibit a good fit with the measured mass loss curves.

The results for all materials are given in Table 3. Values for the  $A$  parameter are all in the E-14 m<sup>2</sup>/s range. The values estimated from the drying test results are related to the quality of the materials tests. The lowest value was obtained with the fly-ash concrete (material E). The parameter  $A$  increased progressively with the water/cement ratio of the materials to reached its maximum value for material D, which has a w/c ratio of 0.75.

## 5. Sensitivity analysis

Due to the small thickness of the concrete samples (1 cm) used to determine the equilibrium water content at 50% RH, the estimation of this parameter can yield imprecise values. Averaging measurements on three samples may not be enough to eliminate the expected uncertainty on such small test specimens. A sensitivity analysis was thus performed to estimate the impact of variations in  $w_{eq}$  on the drying test modeling. The study was based on the calculation of the elasticity of the model parameters. The elasticity provides an estimation of the relative importance of variations of parameters on the output of a model. It is calculated as:

$$\eta = \frac{\Delta Y \bar{P}}{\Delta P \bar{Y}} \quad (21)$$

where  $\bar{Y}$  is the output of the model calculated with parameter  $\bar{P}$  and  $\Delta Y$  is the variation in the output of the model with input parameter variation of  $\Delta P$ .

Data from material A (w/c:0.4, Type 10 cement concrete) in Table 3 were used for the calculations. The input parameters considered for the calculations are:  $A$ ,  $\phi$ ,  $h$  and  $w_{eq}$ . The parameter  $B$  was not considered since it was fixed at 80. The calculations are performed over 50 mm using Richards' model (eq. (13)) with Cauchy boundary conditions (19). The previous parameters are varied one at a time. The variation used in this study is  $\pm 5\%$ . In this case,  $\bar{P}/\Delta P = 10.0$ . The output considered for the analysis is the mass loss after 90 days of drying. The value of the mass loss using the parameters for material A in Table 3 is 14.136 g after 90 days.

The results of the sensitivity analysis are presented in Table 4. They show that the model is very sensitive to the porosity value, while it is much less sensitive to variations of parameters  $A$  and  $w_{eq}$ . At the other end of the spectrum, the model showed a very weak sensitivity to the parameter  $h$ . The strong dependence on porosity indicates that special attention must be given to the estimation of this parameter using the ASTM C642 procedure. On the other hand, a separate study made by one coauthor showed that a 5% uncertainty in porosity measurements is expected using this procedure<sup>10</sup>. The measurement of porosity is thus not subject to strong variations and is reliable. Because the elasticity of  $w_{eq}$  is 7.5 times lower than the elasticity of porosity, errors made on this parameter estimation have much less impact on the overall response of the model and are not detrimental to the analysis. Finally, even though very few studies have been published on the estimation of the exchange parameter  $h$  and its dependence on the type of material and the exposure conditions, its weak elasticity indicates that it has a very small impact on the drying test analysis.

## 6. Parameter validation

To validate the value of the parameters obtained with the drying tests, the samples were submitted to different exposure and test conditions. The parameters  $A$  and  $B$  were then used to reproduce the measured mass change curves.

The first case consisted in placing the three samples per series in water at the end of the drying test, to see if the parameters could be used to simulate structures exposed to wetting/drying cycles. The samples were weighed under water during absorption to avoid errors associated with the presence of water on the surface of the disks. The mass was measured regularly and plotted on the graph with the drying data (Figure 6). The absorption thus corresponds to a drop on the mass loss axis. The absorption was then simulated with Richards' equation (13) using the parameters  $A$  and  $B$  evaluated from the drying tests. To simulate contact with water, a Dirichlet boundary condition was approximated by a Cauchy boundary condition (equation (19)), with  $w_{eq} = \phi$  and an exchange coefficient  $h_w$  1000 times

---

<sup>10</sup> Unpublished data.

higher than for drying. In theory, a Dirichlet condition corresponds to  $h_w \rightarrow \infty$ . However, an exchange coefficient 1000 times higher proved sufficient. The results are shown on Figure 6. Overall, the model provides a good match with the mass variations measured during absorption. In the example shown on Figure 6, the samples from the 1-cm series were subjected to another drying sequence after absorption and the model successfully reproduced the experimental mass loss. It is thus possible to simulate wetting and drying cycles using Richards' model and an exponential water diffusivity evaluated from drying test results.

The next tests consisted in performing a drying test on 10-cm thick samples. The experimental procedure described in section 3 was followed. Again, three samples were used. The parameters evaluated from the 1-cm and 5-cm test series were then used to simulate the mass loss of these larger samples. Figure 7 shows the results obtained for concrete mixture E (fly ash mixture), using the parameters listed in Table 3. The numerical simulation shows that the drying kinetics of the 10-cm samples is reproduced correctly, thus showing the possibility of using the water diffusivity to estimate the water content profiles on larger structures.

The last series of test focused on the long-term kinetic of the drying process. To achieve this, samples were kept in the 50% RH room after the 1-cm series had reached equilibrium. The mass of the three disks was measured twice per week until 120 days of drying and once per week after that. A simulation was made to reproduce the average mass loss of the three disks using the water diffusivity parameters estimated upon reaching the equilibrium of the 1-cm series after approximately 80 days (see Table 3). The simulation results are shown on Figure 8 for the fly ash concrete mixture and show a good agreement with the measured data after over 180 days of drying. The experimental results on Figure 8 exhibit a rapid change in drying rate around 40 days. This was due to a malfunction of the chamber, where the humidity dropped to 35% for three days.

Looking at Figure 5 to 8, one could argue that the model does not properly fit the measured mass loss curves. However, it is important to put the results in perspective. On Figure 8, the mass loss predicted by the model after 180 days is 8.3g, compared to a measured value of 7.7g, an acceptable difference of 7.8%. Moreover, most wetting/drying cycle periods for concrete structures are much shorter than that, which means that in most real-life cases, the water diffusivity obtained with this method should provide a reliable estimation of the water content in cementitious materials.

## 7. Conclusion

The paper presented a new method for evaluating the water diffusivity of cementitious materials. It is based on the results of drying tests performed on samples with 1-cm and 5-cm thicknesses. The analysis is performed using Richards' water transport model, under the assumption that the water diffusivity can be expressed as an exponential function:  $D_w = A \exp(Bw)$ . The test results showed that it is possible to use a constant value

of 80 for B, which leaves  $A$  to be determined. It is obtained by minimizing the error between the numerical and measured mass loss curves for both 1-cm and 5-cm series.

The water diffusivity evaluated from this method was used to predict the mass variation of samples exposed to different test conditions. It proved its ability to predict drying over and extended period of time and on larger samples. Most importantly, it was shown that the water diffusivity can be used to reproduce absorption cases, which make it suited to model service-life of structures exposed to wetting/drying cycles.

## 8. Acknowledgements

The authors are thankful for the contribution of Yannick Protière (Laval University), who provided the 14-month equilibrium data presented in section 4.

## 9. References

- [1] Ghods P., Chini M., Alizadeh R., Hoseini M. (2005). "The effect of different exposure conditions on the chloride diffusion into concrete in the Persian Gulf region", in Proceedings of the ConMAT Conference, N. Banthia et al. eds., Vancouver (Canada).
- [2] Saetta, A., Scotta, R. and Vitaliani, R., 'Analysis of chloride diffusion into partially saturated concrete', *ACI Materials Journal*. 90(5) (1993) 441-451.
- [3] Nagesh, M. and Bhattacharjee, B., 'Modeling of chloride diffusion in concrete and determination of diffusion coefficients', *ACI Materials Journal*. 95(2) (1998) 113-120.
- [4] Hansen, E.J. and Saouma V.E., 'Numerical simulation of reinforced concrete deterioration – part 1: chloride diffusion', *ACI Materials Journal*. 96(2) (1999) 173-180.
- [5] Swaddiwudhipong, S., Wong, S.F., Wee, T.H. and Lee, S.L., 'Chloride ingress in partially and fully saturated concrete structures', *Concrete Science and Engineering*. 2 (2000) 17-31.
- [6] Martin-Perez, B., Pantazopoulou, S.J. and Thomas, M.D.A., 'Numerical solution of mass transport equations in concrete structures', *Computers and Structures*. 79 (2001) 1251-1264.
- [7] Masi, M., Colella D., Radaelli, G. and Bertolini L., 'Simulation of chloride penetration in cement-based materials', *Cement and Concrete Research*. 27(10) (1997) 1591-1601.

- [8] Samson E., Marchand J. (2007). "Modeling the effect of temperature on ionic transport in cementitious materials", *Cement and Concrete Research*, vol. 37, p. 455-468.
- [9] McGrath P.F., Hooton R.D., Influence of voltage on chloride diffusion coefficients from chloride migration tests, *Cement and Concrete Research* 26 (1996) 1239-1244.
- [10] Tong L., Gjørsv O.E., Chloride diffusivity based on migration testing, *Cement and Concrete Research* 31 (2001) 973-982.
- [11] Samson E., Marchand J., Snyder K.A., *Calculation of ionic diffusion coefficients on the basis of migration test results*, *Materials and Structures*, vol.36, p.156-165, 2003.
- [12] Friedmann H., Amiri O., Aït-Mokhtar A., Dumargue P., A direct method for determining chloride diffusion coefficient by using migration test, *Cement and Concrete Research* 34 (2004) 1967-1973.
- [13] Pel L., Kopinga K., Brocken H., Determination of moisture profiles in porous building materials by NMR, *Magnetic Resonance Imaging* 7/8 (1996) 931-932.
- [14] Carmeliet J., Hens H. Roels S., Adan O. et al., Determination of the liquid water diffusivity from transient moisture transfer experiments, *Journal of Thermal Envelope and Building Science* 27 (2004) 277-305.
- [15] Mainguy M., Coussy O., Baroghel-Bouny V., Role of Air Pressure in Drying of Weakly Permeable Materials, *Journal of Engineering Mechanics* 127 (2001) 582-592.
- [16] Degiovanni A., Moyne C., Conductivité thermique de matériaux poreux humides: évaluation théorique et possibilité de mesure, *Int. J. Heat Mass Transfer* 30 (1987) 2225-2245 (in French).
- [17] Selih J., Sousa A.C.M., Bremner T.W., Moisture transport in initially fully saturated concrete during drying, *Transport in porous media* 24 (1996) 81-106.
- [18] Whitaker S., Coupled transport in multiphase systems: a theory of drying, in *Advance in Heat Transfer* 31, J.P. Hartnett et al. eds. (1998) 1-104.
- [19] Samson, E., Marchand, J., Snyder, K.A. and Beaudoin, J.J., Modeling ion and fluid transport in unsaturated cement systems in isothermal conditions, *Cement and Concrete Research* 35 (2005) 141-153.
- [20] Hall C., Barrier performance on concrete: a review of fluid transport theory, *Materials and Structures* 27 (1994) 291-306.



- [21] Bazant Z.P., Najjar L.J., Drying of concrete as a nonlinear diffusion problem, *Cement and Concrete Research* 1 (1971) 461-473.
- [22] Xi Y., Bazant Z.P., Molina L., Jennings H.M., Moisture diffusion in cementitious materials - Moisture capacity and diffusivity, *Advanced Cement Based Materials* 1 (1994) 258-266.
- [23] J. Bear, Y. Bachmat, *Introduction to Modeling of Transport Phenomena in Porous Media*, Kluwer Academic Publishers, The Netherlands, 1991.
- [24] Sakata K., A study of moisture diffusion in drying and drying shrinkage of concrete, *Cement and Concrete Research* 13 (1983) 216-224.

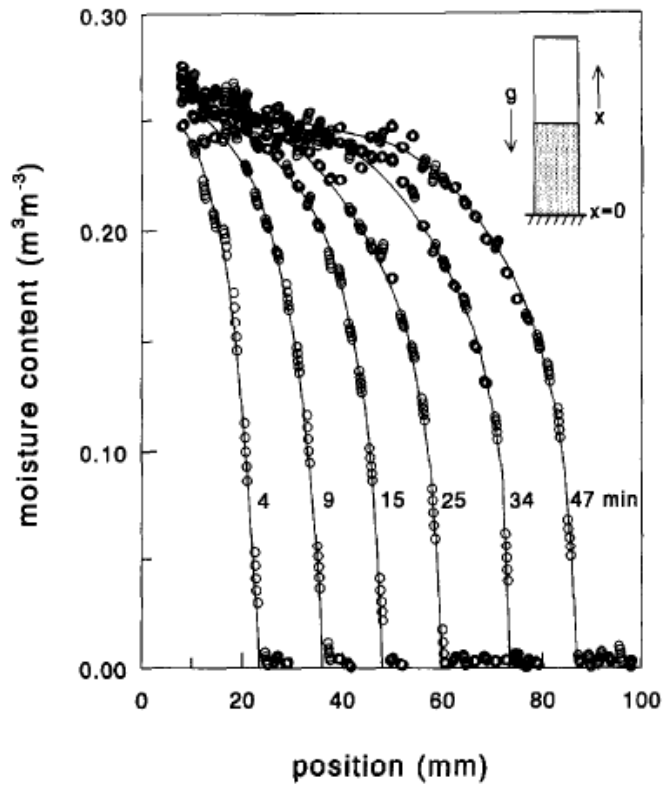


Figure 1 – Water content profiles measured using the NMR technique [Pel96]

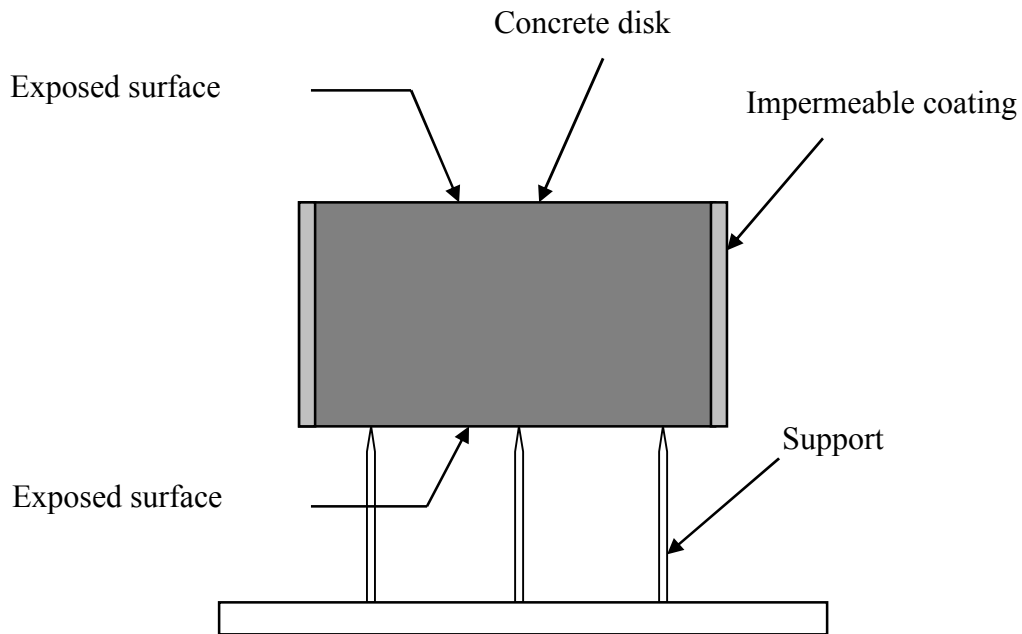


Figure 2 – Drying test set-up

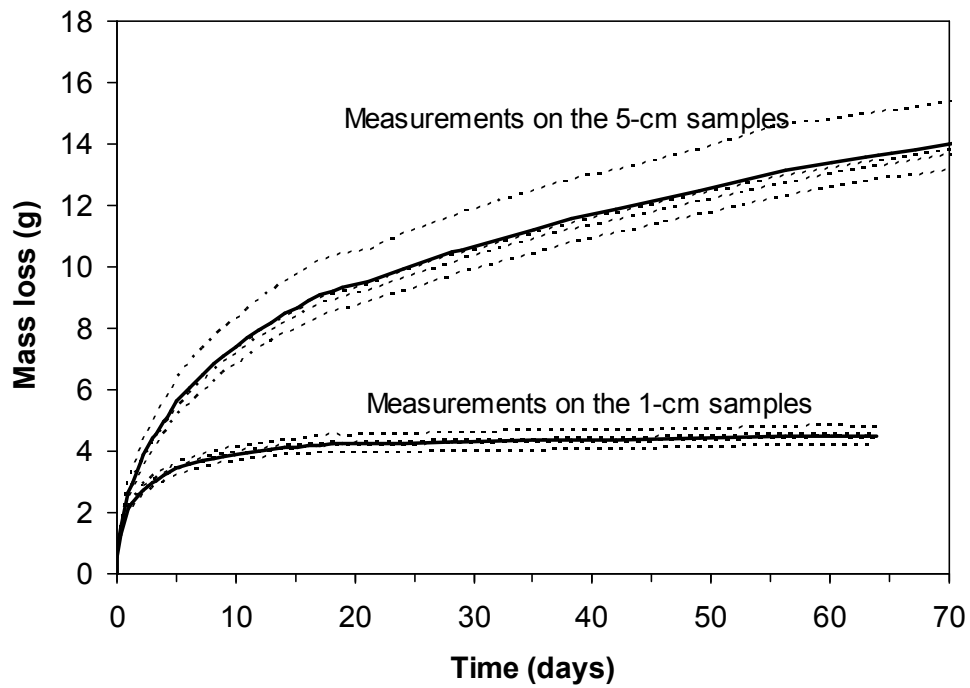


Figure 3 – Mass loss measured from the 0.4 w/c CSA Type 10 concrete. The thick lines correspond to the average measurements.

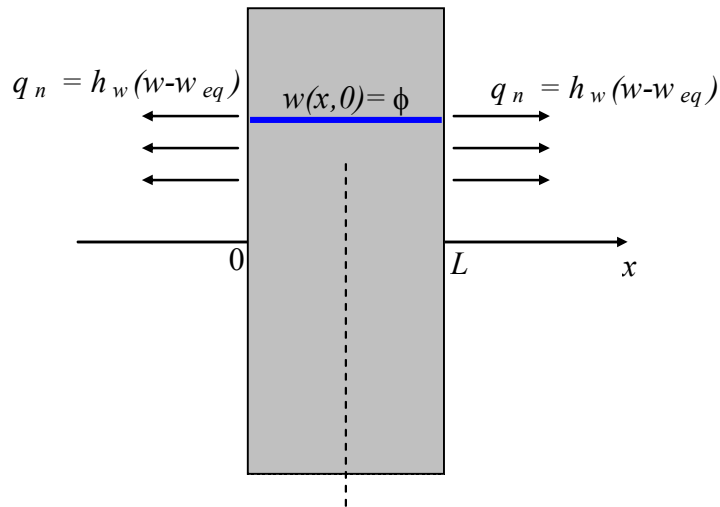


Figure 4 – Simulation initial and boundary conditions for the test analysis.

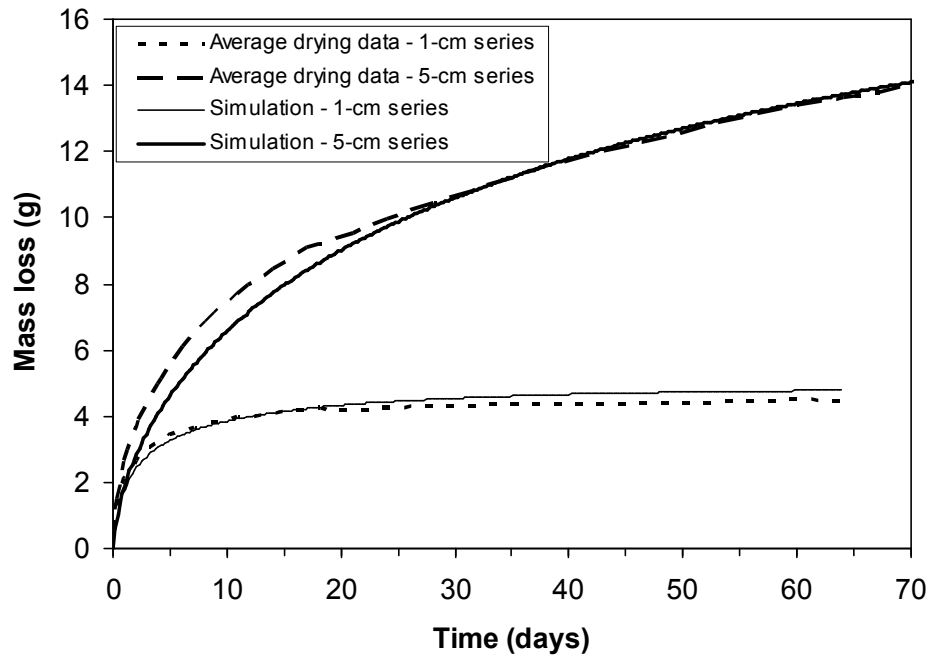


Figure 5 – Drying simulations for material A. The best fit with the measured values was obtained with  $A=1.41 \times 10^{-14} \text{ m}^2/\text{s}$ .

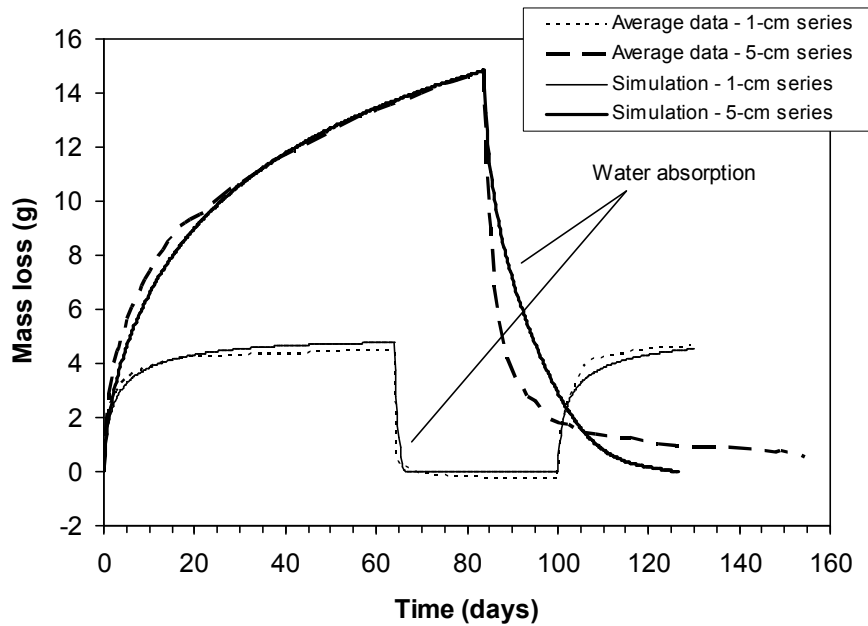


Figure 6 – Mass loss curve for material A (0.4 Type 10 concrete) exposed to water after the drying test.

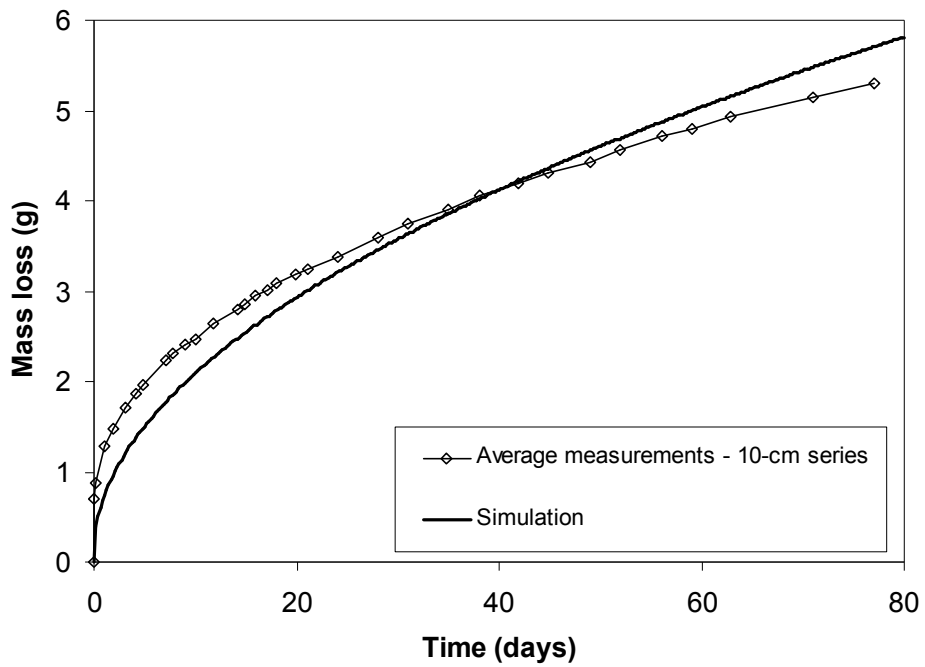


Figure 7 – Mass loss curve for a drying test performed on 10-cm samples made with material E (0.35 Type I concrete with fly ash).

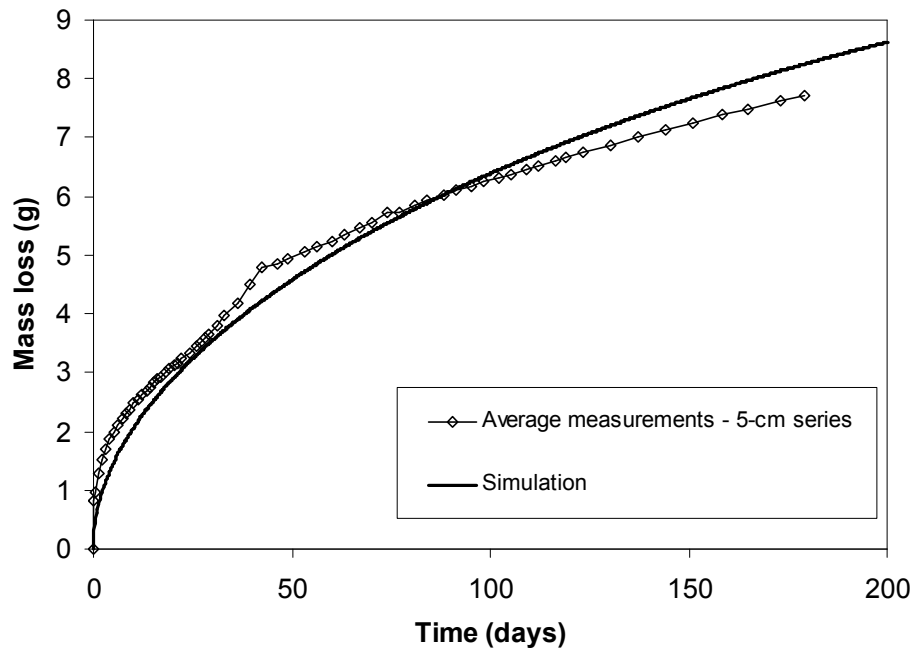


Figure 8 – Mass loss curve for material E (fly ash mixture) for the drying test on the 5-cm series performed over an extended period of time.

Table 1 – Mixture characteristics.

Characteristics	Concrete series				
	A	B	C	D	E
W/B	0.4	0.5	0.65	0.75	0.35
Cement Type	CSA Type 10	CSA Type 10	CSA Type 10	CSA Type 10	ASTM Type I
Cement (kg/m <sup>3</sup> )	410	380	280	250	340
Fly Ash F (kg/m <sup>3</sup> )	–	–	–	–	85
Sand (kg/m <sup>3</sup> )	770	765	840	865	810
Coarse aggregates (kg/m <sup>3</sup> )	960	1035	1065	1050	920

Table 2 – Verification of the equilibrium water content for the drying tests.

Material	Water content at 50% RH (m <sup>3</sup> /m <sup>3</sup> )	
	Drying tests	Equilibrium tests
B	0.062	0.063
C	0.053	0.046
D	0.051	0.048

Table 3 – Analysis results.

Materials	Porosity (m <sup>3</sup> /m <sup>3</sup> )	$w_{eq}$ (m <sup>3</sup> /m <sup>3</sup> )	$h_w$ (m/s)	B (1)	A (m <sup>2</sup> /s)
A	0.1306	0.078	$10 \times 10^{-8}$	80.0	$1.4 \times 10^{-14}$
B	0.1310	0.062	$10 \times 10^{-8}$	80.0	$2.5 \times 10^{-14}$
C	0.1340	0.053	$10 \times 10^{-8}$	80.0	$12.1 \times 10^{-14}$
D	0.1390	0.051	$10 \times 10^{-8}$	80.0	$26.5 \times 10^{-14}$
E	0.1088	0.065	$10 \times 10^{-8}$	80.0	$0.8 \times 10^{-14}$

Table 4 – Results of the sensitivity analysis

Parameter	Mass loss (g)		$\frac{\Delta Y}{\bar{Y}}$	$\eta$
	$\bar{P}+5\%$	$\bar{P}-5\%$		
$A$	14.313	13.948	0.0258	0.258
$\phi$	16.589	11.745	0.3427	3.427
$h$	14.138	14.134	2.83E-4	2.83E-3
$w_{eq}$	13.781	14.422	0.0453	0.453

**BLANK PAGE**

**DISTRIBUTION:**

A. B. Barnes, 999-W  
H. H. Burns, 999-W  
T. W. Coffield, 766-H  
A. D. Cozzi, 999-A  
D. A. Crowley, 773-43A  
R. D. Deshpande, 766-H  
M. E. Dehnam, Jr., 773-42A  
K. L. Dixon, 773-42A  
G. P. Flach, 773-42A  
J. C. Griffin, 773-A  
E. K. Hansen, 999-W  
J. R. Harbour, 999-W  
C. C. Herman, 999-W  
M. H. Layton, 766-H  
J. E. Marra, 773-A  
S. L. Marra, 773-A  
J. L. Newman, 766-H  
M. A. Phifer, 773-42A  
T. C. Robinson, 766-H  
L. B. Romanowski, 766-H  
K. H. Rosenberger, 7766-H  
R. R. Seitz, 773-43A  
E. L. Wilhite, 773-43A